ALK1 regulates the internalization of endoglin and the type III TGF-β receptor

Keren Tazat[a,†], Leslie Pomeraniec-Abudy[a,†], Melissa Hector-Greene[b,†], Szabina Szófia Szilágyi[a], Swati Sharma[a], Elise M. Cai[b], Armando L. Corona[b], Marcelo Ehrlich[c], Gerard C. Blobe[b], and Yoav I. Henis[a,*]

[a]Department of Neurobiology and [c]Department of Cell Research and Immunology, George S. Wise Faculty of Life Sciences, Tel Aviv University, Tel Aviv 6997801, Israel; [b]Department of Medicine, Duke University Medical Center, Durham, NC 27708

ABSTRACT **Complex formation and endocytosis of transforming growth factor-β (TGF-β) receptors play important roles in signaling. However, their interdependence remained unexplored. Here, we demonstrate that ALK1, a TGF-β type I receptor prevalent in endothelial cells, forms stable complexes at the cell surface with endoglin and with type III TGF-β receptors (TβRIII). We show that ALK1 undergoes clathrin-mediated endocytosis (CME) faster than ALK5, type II TGF-β receptor (TβRII), endoglin, or TβRIII. These complexes regulate the endocytosis of the TGF-β receptors, with a major effect mediated by ALK1. Thus, ALK1 enhances the endocytosis of TβRIII and endoglin, while ALK5 and TβRII mildly enhance endoglin, but not TβRIII, internalization. Conversely, the slowly endocytosed endoglin has no effect on the endocytosis of either ALK1, ALK5, or TβRII, while TβRIII has a differential effect, slowing the internalization of ALK5 and TβRII, but not ALK1. Such effects may be relevant to signaling, as BMP9-mediated Smad1/5/8 phosphorylation is inhibited by CME blockade in endothelial cells. We propose a model that links TGF-β receptor oligomerization and endocytosis, based on which endocytosis signals are exposed/functional in specific receptor complexes. This has broad implications for signaling, implying that complex formation among various receptors regulates their surface levels and signaling intensities.**

Monitoring Editor
Kunxin Luo
University of California, Berkeley

Received: Mar 19, 2020
Revised: Jan 4, 2021
Accepted: Feb 1, 2021

This article was published online ahead of print in MBoC in Press (http://www.molbiolcell.org/cgi/doi/10.1091/mbc.E20-03-0199) on February 10, 2021.

†These authors contributed equally to this work.

ORCID 0000-0002-1408-3877.

*Address correspondence to: Yoav I. Henis (henis@post.tau.ac.il).

Abbreviations used: BSA, bovine serum albumin; BMP, bone morphogenetic protein; CME, clathrin-mediated endocytosis; *D*, lateral diffusion coefficient; DαC, donkey anti-chicken; DαM, donkey anti-mouse; DαR, donkey anti-rabbit; DSS, disuccinimidyl suberate; ECs, endothelial cells; FRAP, fluorescence recovery after photobleaching; GαM, goat anti-mouse; GαR, goat anti-rabbit; GIPC, GAIP-interacting protein C-terminal; HHT, hereditary hemorrhagic telangiectasia; MEECs, murine embryonic endothelial cells; NTC, nontargting control; R_f, mobile fraction; TGF-β, transforming growth factor-β; TβRII, TβRIII, type II and III TGF-β receptors; WT, wild type.

© 2021 Tazat, Pomeraniec-Abudy, Hector-Greene, *et al*. This article is distributed by The American Society for Cell Biology under license from the author(s). Two months after publication it is available to the public under an Attribution–Noncommercial–Share Alike 3.0 Unported Creative Commons License (http://creativecommons.org/licenses/by-nc-sa/3.0).

"ASCB®," "The American Society for Cell Biology®," and "Molecular Biology of the Cell®" are registered trademarks of The American Society for Cell Biology.

INTRODUCTION

The transforming growth factor-β (TGF-β) superfamily ligands regulate diverse physiologic and pathologic cellular processes, which in endothelial cells (ECs) include migration and angiogenesis, and were implicated in the development of diseases such as hereditary hemorrhagic telangiectasia (HHT) (McAllister *et al*., 1994; Johnson *et al*., 1996; Bourdeau *et al*., 1999; Lebrin *et al*., 2005; Goumans *et al*., 2009; McDonald *et al*., 2015; Roman and Hinck, 2017). They exert their effects through ligand-receptor interactions, mediated via type I and type II dual-specificity (Ser/Thr and Tyr) kinase receptors (Shi and Massague, 2003; Derynck and Miyazono, 2008; Ehrlich *et al*., 2012; Heldin and Moustakas, 2016). In ECs, typical type I receptors are ALK5 (which acts with the TGF-β–responsive type II TGF-β receptor, TβRII) and ALK1 (which can interact with several type II receptors, including TβRII, and BMP9/10-responsive type II receptors for activin or bone morphogenetic proteins [BMPs]) (Oh *et al*., 2000; Seki *et al*., 2003; Lebrin *et al*., 2004, 2005;

Roman and Hinck, 2017). In general, ligand binding to type II and type I receptors triggers phosphorylation and activation of the type I receptor, which phosphorylates specific R-Smads, followed by their association with Smad4 and accumulation in the nucleus, where they regulate transcription (Shi and Massague, 2003; Feng and Derynck, 2005; Schmierer and Hill, 2007; Heldin *et al.*, 2009; Budi *et al.*, 2017). TGF-β stimuli in ECs can activate Smad2/3 and Smad1/5/8 via ALK5 and ALK1, respectively (Chen and Massague, 1999; Goumans *et al.*, 2003; Shi and Massague, 2003; Lebrin *et al.*, 2005; Moustakas and Heldin, 2009), and ALK1 activation by BMP9 or BMP10 signal via Smad1/5/8 (Lebrin *et al.*, 2004). ALK1 activity was shown to be essential for vascular development, as ALK1 knockout mice exhibit embryonic lethality at day 10.5 due to defective angiogenesis (Oh *et al.*, 2000; Srinivasan *et al.*, 2003), and ALK1 is often mutated in HHT (Johnson *et al.*, 1996; Lebrin *et al.*, 2005). ALK1 heterozygous mice phenocopy this multisystemic vascular dysplasia syndrome (Oh *et al.*, 2000; Urness *et al.*, 2000). In spite of the biological significance of ALK1 signaling, and the controversy on the potential roles for TGF-β superfamily receptor trafficking in regulating signal output (Ehrlich *et al.*, 2001; Penheiter *et al.*, 2002; Di Guglielmo *et al.*, 2003; Mitchell *et al.*, 2004; Shapira *et al.*, 2012; Amsalem *et al.*, 2016; Ehrlich, 2016), the internalization of ALK1 and its potential modulation by interactions with other TGF-β receptors remain to be explored.

TGF-β superfamily signaling can be modulated by several coreceptors. The most abundant are the type III TGF-β receptor (TβRIII) and endoglin (Jonker and Arthur, 2002; Goumans *et al.*, 2003; Lebrin *et al.*, 2005; Bernabeu *et al.*, 2009; Mahmoud *et al.*, 2009; Gatza *et al.*, 2010). While endoglin is known to be coexpressed in ECs along with ALK1, this was unclear for TβRIII, which was reported to be found in cardiac ECs and in some microvascular but not macrovascular bovine ECs (Morello *et al.*, 1995; Brown *et al.*, 1999), and which we now find to be expressed in multiple EC cell types (Figure 1). TβRIII is a proteoglycan that binds several ligands, including TGF-βs, inhibin, and some BMPs, and presents them to the signaling receptors (Lopez Casillas *et al.*, 1994; Kirkbride *et al.*, 2008). It

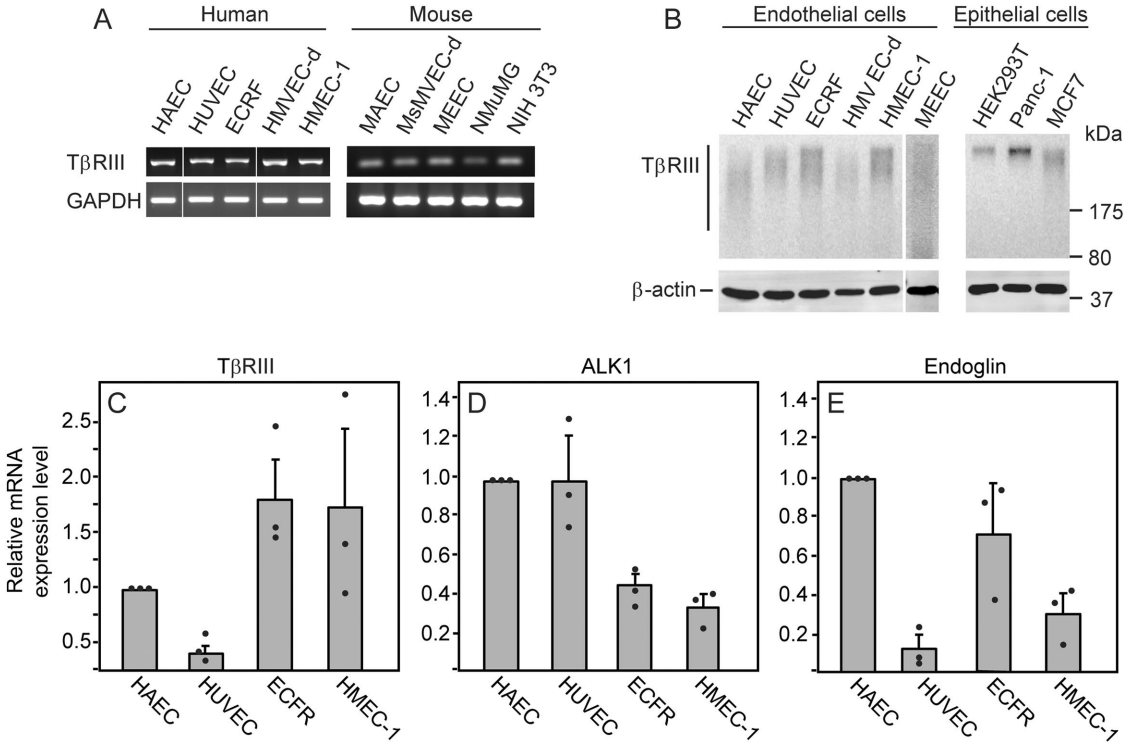

FIGURE 1: Expression of TβRIII, endoglin, and ALK1 in human and murine cell lines. (A, B) TβRIII is expressed in human and murine ECs. The various cell lines were grown in six-well plates and subjected to experiments to determine TβRIII mRNA (A) or protein (B) expression. Authentication of all immortalized human cell lines was carried out by short tandem repeat analysis at the Duke University DNA Analysis Sequencing Facility. (A) RT-PCR of TβRIII in human and murine cells. RNA isolation was followed by conversion to cDNA and RT-PCR (see *Materials and Methods*). GAPDH cDNA levels are shown as control. A representative experiment ($n = 3$) is shown. TβRIII mRNA expression is demonstrated for human ECs of arterial (HAEC; cat. #CC-2535; Lonza, Basel, Switzerland), venous (HUVEC and ECRF, gifts from C. Kontos, Duke University, Durham, NC, and R. Fontijn, Academic Medical Centre, Amsterdam, the Netherlands, respectively), and microvascular (HMEC-1 [cat. #CRL-3243; ATCC] and HMVEC-d [cat. #CC-2543; Lonza) origin, as well as for murine ECs of arterial (MAEC; a gift from C. Kontos), microvascular (MsMVEC-d, obtained from D. Kirsch, Duke University, Durham, NC), and embryonal (MEEC) origin. Non-ECs (NMuMG [cat. #CRL-1636 ATCC] and NIH3T3 [cat. #CRL-1658; ATCC]) were included for comparison. (B) Cell surface TβRIII was detected by [^{125}I]TGF-β1 binding/cross-linking followed by immunoprecipitation as described under *Materials and Methods*. Non-ECs (HEK293T [cat. #CRL-3216; ATCC], Panc-1 [cat. #CRL-1469; ATCC], and MCF7 [obtained from the Michigan Cancer Foundation]) were included for comparison. Data are representative of three experiments. (C–E) RT-qPCR quantification of TβRIII (C), ALK1 (D), and endoglin (E) in human ECs (HAEK, HUVEC, ECRF, and HMEC-1). Data were normalized to the cDNA levels of GAPDH, taking the value of the mRNA transcript measured in HAEC cells as 1 (see *Materials and Methods*). The results are the mean ± SEM of three independent experiments, each conducted in triplicate.

can also modulate signaling by forming mutual complexes with the signaling receptors (Henis *et al.*, 1994; Lopez Casillas *et al.*, 1994; Eickelberg *et al.*, 2002; reviewed in Gatza *et al.*, 2010). In this context, we have recently shown (Tazat *et al.*, 2015) that ALK5 and TβRII bind to TβRIII simultaneously but not as a complex, competing with ALK5-TβRII signaling complex formation and thus inhibiting TGF-β–mediated Smad signaling in MDA-MB-231 cells. TβRIII was shown to have a role in developmental angiogenesis in a zebrafish model (Kamaid *et al.*, 2015). In mammals, it is important for vasculogenesis, as TβRIII knockout mice are embryonic lethal at day 14.5 due to defective vasculogenesis (Compton *et al.*, 2007). Endoglin, the most abundant TGF-β superfamily coreceptor in ECs, regulates differentiation and angiogenesis (Li *et al.*, 1999; Arthur *et al.*, 2000), and mutations in endoglin cause HHT1 (McAllister *et al.*, 1994; Lebrin *et al.*, 2005). At the cell surface, endoglin can bind TGF-β1/3 and BMP9/10 (and other BMPs to a lesser extent) and can interact with signaling TGF-β superfamily receptors (Bernabeu *et al.*, 2009; Alt *et al.*, 2012). In this context, employing quantitative studies that measure directly the receptors' interactions at the cell surface, we have demonstrated that endoglin functions as a scaffold for binding TβRII, ALK5, and ALK1, thus regulating the balance between TGF-β signaling to Smad1/5/8 and to Smad2/3 (Pomeraniec *et al.*, 2015).

The cell surface levels of TβRIII and endoglin were reported to be affected by diverse cellular processes and experimental manipulations. Thus, alteration of the β-arrestin2 expression level was shown to affect the cell surface localization of both TβRIII (Chen *et al.*, 2003; Finger *et al.*, 2008; McLean and Di Guglielmo, 2010) and endoglin (Lee and Blobe, 2007), suggesting regulation of their intracellular distribution by endocytosis. The endocytic pathways involved remained controversial (Finger *et al.*, 2008; McLean and Di Guglielmo, 2010), largely due to measurement of receptor down-regulation rather than internalization per se. Importantly, the kinetics of the endocytosis of these receptors and their modulation by interactions with the signaling TGF-β receptors remained unexplored. In the current paper, we employed biophysical studies on epitope-tagged TGF-β receptors to demonstrate that ALK1 forms stable complexes at the cell surface with TβRIII, as we reported formerly for ALK1-endoglin interactions (Pomeraniec *et al.*, 2015). Using quantitative point-confocal microscopy for direct endocytosis measurements, we found that ALK1 undergoes fast clathrin-mediated endocytosis (CME), significantly faster than that of ALK5 or TβRII, and much faster than TβRIII and endoglin. Of note, we show that the interactions between ALK1 and TβRIII or endoglin enhance the endocytosis rates of the latter two receptors, while TβRIII (but not endoglin) inhibits the internalization of ALK5 and TβRII. These phenomena correlate with the blockade of BMP9-mediated signaling to Smad1/5/8 by inhibition of CME but not by nystatin in murine embryonic endothelial cells (MEECs). We propose a model that links TGF-β receptors complex formation with their endocytosis, based on which endocytosis signals are exposed (available for binding to the endocytosis machinery) in the specific receptor complex, with potential implications for signaling regulation.

RESULTS

ALK1 forms stable heteromeric complexes with TβRIII

ALK1 and endoglin are characteristically expressed in ECs (Jonker and Arthur, 2002; Seki *et al.*, 2003; Lebrin *et al.*, 2004, 2005; Bernabeu *et al.*, 2009; Mahmoud *et al.*, 2009; Roman and Hinck, 2017). They were shown to interact with each other (Bernabeu *et al.*, 2009; Alt *et al.*, 2012), and ALK1 at the surface of live cells was shown to form stable complexes with itself and with endoglin (Pomeraniec *et al.*, 2015). TβRIII was also reported to be expressed in some ECs (Morello *et al.*, 1995; Brown *et al.*, 1999). As shown in Figure 1, A and B, we find TβRIII expression in multiple types of human and murine ECs, as well as in epithelial cell lines. Comparison between the mRNA expression levels of TβRIII, endoglin, and ALK1 in several human EC lines by real-time quantitative reverse-transcriptase PCR (RT-qPCR) showed that they express the mRNA transcripts for all three proteins, but at different levels (Figure 1, C–E). In view of the interactions between ALK1 and endoglin, it was important to explore whether ALK1 and TβRIII interact. To this end, we initially coexpressed extracellularly tagged HA-ALK1 (wild type [WT], constitutively active Q201D, or kinase-dead K221R) together with myc-TβRIII. Immunoprecipitation of myc-TβRIII resulted in coprecipitation of all the HA-ALK1 variants (Figure 2, A and B), suggesting that the two receptors interact irrespective of ALK1 kinase activity. Of note, the high-molecular-weight smear of the heavily glycosylated TβRIII is more difficult to detect at low expression levels, and the failure to detect it in the immunoprecipitated TβRIII bands may suggest that the two receptors interact already at the endoplasmic reticulum (ER), yielding coimmunoprecipitation, which includes a significant contribution from the ER population. This interpretation is in line with the enrichment in the lower band of HA-ALK1 coprecipitated with TβRIII, which most likely represents its ER form. Nevertheless, the two receptors interact also at the cell surface, as indicated by the experiments shown in Figure 2, C–F.

To measure the interactions between TβRIII and ALK1 at the plasma membrane in live cells, we employed the patch/FRAP (fluorescence recovery after photobleaching) method, which measures interactions between receptors situated at the cell surface (Henis *et al.*, 1990; Rechtman *et al.*, 2009; Pomeraniec *et al.*, 2015; Tazat *et al.*, 2015). In this method, cross-linking of a tagged receptor by a double layer of immunoglobulins G (IgGs) results in its patching and lateral immobilization. The effects of this immobilization on the lateral diffusion of a coexpressed, differently tagged receptor labeled exclusively by monovalent Fab' fragments are then measured by FRAP (see *Materials and Methods*). The nature of the effect depends and reports on the extent and mode of mutual complex formation between the receptors. Complex lifetimes longer than the characteristic FRAP times (interactions that are stable at this time range) are reflected by a reduction in the mobile fraction (R_f), because bleached Fab'-labeled receptors associated with cross-linked, immobilized receptors do not appreciably dissociate from the immobile patches during the FRAP measurement. On the other hand, transient complexes (short complex lifetimes) would lead to multiple association–dissociation cycles during the FRAP measurement, resulting in a reduced apparent diffusion rate (D), without affecting R_f (Henis *et al.*, 1990; Eisenberg *et al.*, 2006; Rechtman *et al.*, 2009).

In the studies depicted in Figure 2, C–F, myc-TβRIII was laterally mobile when labeled by monovalent Fab' fragments (Figure 2C) and became immobile when cross-linked by IgGs (Figure 2D). Singly expressed HA-ALK1 exhibited lateral mobility similar to other TGF-β superfamily receptors (Yao *et al.*, 2002; Rechtman *et al.*, 2009; Marom *et al.*, 2011; Pomeraniec *et al.*, 2015; Tazat *et al.*, 2015), which is typical of transmembrane proteins (Figure 2, E and F). The lateral diffusion parameters of ALK1 were not affected by TGF-β1 or TGF-β2, while BMP9 induced some reduction in the R_f value, suggesting that BMP9 may induce stable interactions of a fraction of the ALK1 population with other endogenous protein scaffolds/structures. For patch/FRAP studies on TβRIII-ALK1 interactions, we coexpressed HA-ALK1 and myc-TβRIII and investigated the effects of cross-linking myc-TβRIII without and with ligand on HA-ALK1 diffusion. Immobilization of myc-TβRIII induced an ~30% reduction in the R_f of Fab'-labeled HA-ALK1, with no change in D (Figure 2, E and F).

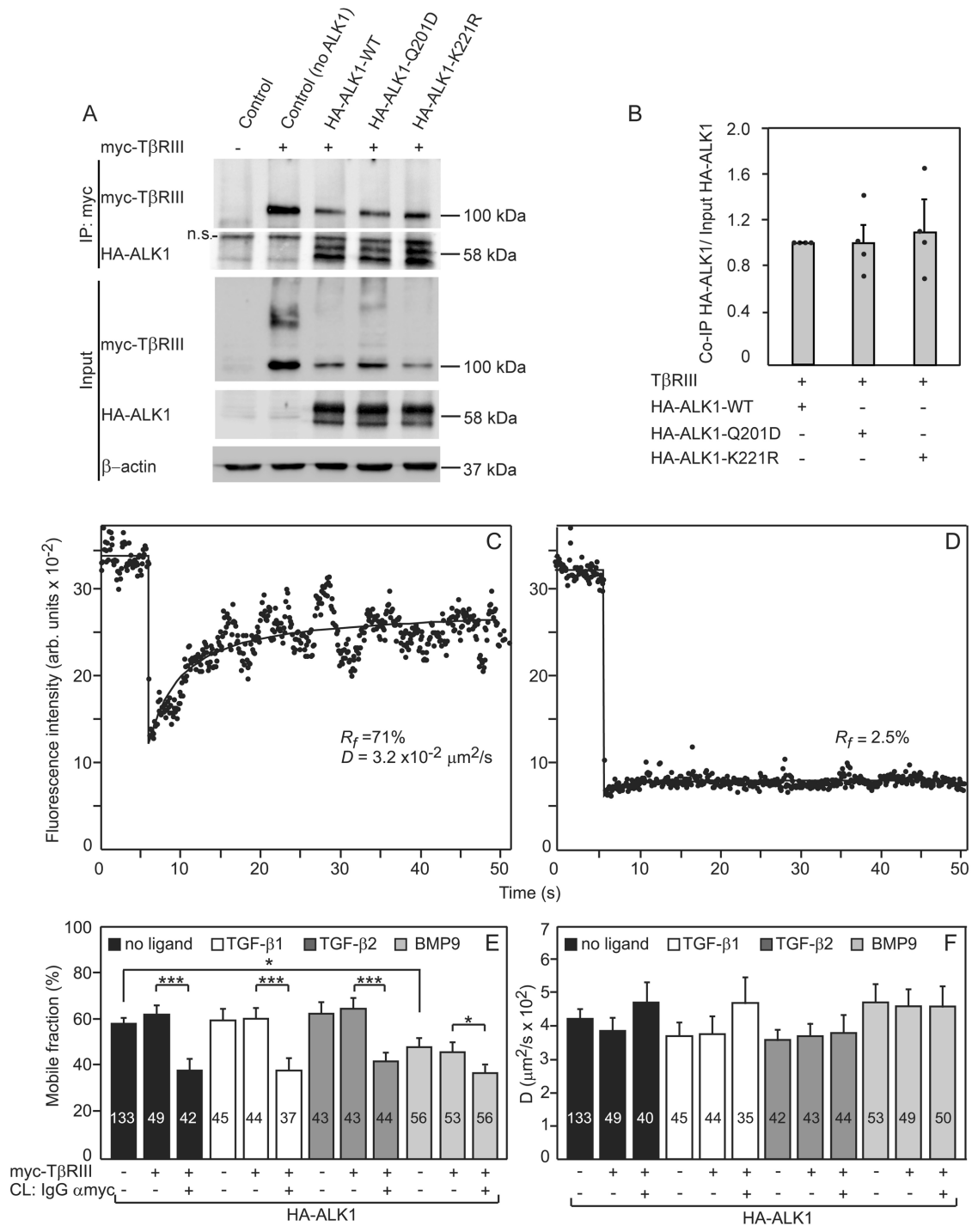

FIGURE 2: Coimmunoprecipitation and patch/FRAP experiments demonstrate that ALK1 and TβRIII form mutual heteromeric complexes. (A) Representative immunoblots of coimmunoprecipitation of HA-ALK1 with myc-TβRIII. COS7 cells were cotransfected with vectors encoding myc-TβRIII and a HA-ALK1 variant (WT, constitutively active [Q201D], or kinase dead [K221R]). Cell lysates were assayed for input of myc-TβRIII (probing the Western blot with murine αmyc) and of HA-ALK1 (using rabbit αHA). The lysates were immunoprecipitated with murine αmyc antibody and assayed for pull down of myc-TβRIII (with murine αmyc) and for HA-ALK1 with rabbit αHA antibody (see *Materials and Methods*). A representative blot ($n = 4$) is shown. The band marked with n.s. for HA-ALK1 is nonspecific. (B) Quantification of the coimmunoprecipitation of HA-ALK1 variants with myc-TβRIII. The bands were quantified (see *Materials and Methods*), and the level of coimmunoprecipitation was determined by dividing the intensity of the band of the coprecipitated HA-ALK1 variant by that of the input of the same HA-ALK1 protein. The value obtained for the coprecipitation of HA-ALK1-WT was defined as 1. There were no significant differences between the coimmunoprecipitation level of the various HA-ALK1 variants ($P > 0.6$; Student's two-tailed t test, $n = 4$). (C) A representative FRAP curve of the lateral diffusion of myc-TβRIII labeled exclusively by Fab′ fragments. (D) Representative FRAP curve of myc-TβRIII immobilized by IgG cross-linking. (E, F) Patch/FRAP studies were carried out on COS7 cells cotransfected with vectors encoding

This effect was not altered by ligand (TGF-β1, TGF-β2, or BMP9). These results indicate that a significant fraction of ALK1 at the cell surface is constitutively and stably associated with TβRIII.

The identification of TβRIII expression in ECs and the demonstration that it forms stable complexes with ALK1 raises the possibility that TβRIII may regulate signaling via ALK1. Because in ECs ALK1 is known to transduce signals initiated by BMP9, leading to Smad phosphorylation and gene transcription changes, we investigated whether TβRIII regulated the ALK1 response to BMP9 in MEECs. To this end, we employed CRISPR to silence TβRIII in MEECs. TβRIII knockout was validated by [^{125}I]TGF-β1 binding and cross-linking (Figure 3A). Loss of TβRIII resulted in a twofold decrease in BMP9-induced pSmad1/5/8 signal (Figure 3, B and C). The attenuation of the response to BMP9 was also apparent in farther downstream signaling, as measured by the reduction in the ability of BMP9 to induce Id1, one of the master regulator genes whose transcription is activated by this pathway (Figure 3D). The reduction in Id1 was modest, in line with the twofold reduction in BMP9-mediated pSmad1/5/8 formation, most likely because the original expression level of TβRIII in the ECs is not very high. Similar to the effect of TβRIII loss on BMP9 signaling to Smad1/5/8 in MEECs, the mild but distinct ability of TGF-β1 to induce pSmad1/5/8 formation was also decreased (Figure 3, E and F). On the other hand, the loss of TβRIII elevated TGF-β1 signaling (mediated via ALK5) to the Smad2/3 pathway (Figure 3, G and H), in line with former reports (Lambert *et al.*, 2011; Tazat *et al.*, 2015). Taken together, these data suggest that TβRIII facilitates ALK1-mediated signaling and downstream functions in ECs, while inhibiting ALK5-mediated Smad2/3 responses.

The short cytoplasmic tail of TβRIII has been demonstrated to interact with β-arrestin2 and GAIP-interacting protein C-terminal (GIPC) (Blobe *et al.*, 2001; Chen *et al.*, 2003). To examine whether the TβRIII cytoplasmic domain or TβRIII glycosylation are required for its interactions with ALK1, we coexpressed HA-TβRIII (WT, the Del mutant lacking the three C-terminal amino acids required to bind GIPC, the T841A point mutant defective in binding β-arrestin2, the ΔGAG mutant lacking the two glycosaminoglycan attachment sites, or the ΔCyto mutant lacking most of the cytoplasmic domain) together with myc-ALK1. To determine quantitatively the association between these HA-TβRIII mutants and myc-ALK1 situated at the plasma membrane, we conducted patch/FRAP studies on cells coexpressing myc-ALK1 and each specific HA-TβRIII variant (Figure 4, A and B). Immobilization of any of the HA-TβRIII mutants reduced the R_f of myc-ALK1 similar to immobilization of WT HA-TβRIII (compare Figures 4A and 2E), with no effect on D of ALK1. We conclude that the stable interactions of ALK1 with TβRIII at the cell surface do not depend on motifs in the TβRIII cytoplasmic domain or on its glycosylation sites. These results are in accord with our studies on endoglin-ALK1 interactions (Pomeraniec *et al.*, 2015), which were also independent of motifs located in the short cytoplasmic tail of endoglin.

ALK1 undergoes fast endocytosis while the internalization of TβRIII and endoglin is slow

Given the detection of interactions of ALK1 with both TβRIII (Figure 2) and endoglin (Pomeraniec *et al.*, 2015) at the cell surface, and the role of endocytosis in regulating surface receptor levels, we next measured the internalization kinetics of ALK1, TβRIII, and endoglin. To this end, we expressed one of these receptors (carrying an extracellular epitope tag), fluorescence labeled the cell surface population of this receptor at 4°C, and followed its endocytosis over time at 37°C by the point-confocal endocytosis assay (Ehrlich *et al.*, 2001; see *Materials and Methods*). The time-dependent internalization of myc-ALK1 was observed as an alteration in its staining pattern from homogeneous to vesicular (Figure 5, A–C). ALK1 endocytosis was quantified by the reduction in the fluorescence intensity at the plasma membrane, measuring the receptor population remaining at the cell surface (Figure 5F). Interestingly, the half-time ($t_{½}$) of ALK1 internalization (2.5 min) was markedly shorter than the $t_{½}$ values for ALK5 (~13 min; Shapira *et al.*, 2012), TβRII (~15 min; Ehrlich *et al.*, 2001), or the type II BMPR receptor (15–20 min; Amsalem *et al.*, 2016). This fast endocytosis is mediated mainly via clathrin-coated pits, as indicated by its inhibition with PitStop 2, which is a specific CME inhibitor (von Kleist *et al.*, 2011), but not with nystatin, an inhibitor of cholesterol-dependent endocytic pathways (Schnitzer *et al.*, 1994; Di Guglielmo *et al.*, 2003) (Figure 5G).

In contrast to the fast endocytosis of ALK1, TβRIII (Figure 6) and endoglin (Figure 7) undergo internalization at much slower rates. Measurements of HA-TβRIII endocytosis by the point-confocal method (Figure 6F) yielded a $t_{½}$ value of 20 min. This value was not affected by ligand (TGF-β1 or BMP9), indicating ligand-independent constitutive endocytosis, in line with earlier reports (Finger *et al.*, 2008; McLean and Di Guglielmo, 2010). TβRIII internalization appears to be mediated mainly via CME, because it was strongly inhibited by PitStop 2 but not by nystatin (Figure 6, D–F). In this context, it should be noted that the TβRIII endocytic pathway is controversial (Finger *et al.*, 2008; McLean and Di Guglielmo, 2010), largely due to measurement of receptor down-regulation rather than internalization per se. The current results using the point-confocal method measure directly and with high sensitivity the internalization of the receptors from the cell surface and suggest a major role of CME in TβRIII endocytosis. In accord with these findings, the cytoplasmic domain of TβRIII is necessary for its endocytosis, as shown by the failure of the HA-TβRIII-ΔCyto mutant to undergo

myc-TβRIII together with HA-ALK1 (or empty vector). The cells were subjected to the IgG cross-linking (CL) protocol that leads to immobilization of myc-TβRIII (protocol 2; *Materials and Methods*), resulting in myc-TβRIII patched and labeled by Alexa 488-DαC IgG (designated "CL: IgG αmyc"), whereas HA-ALK1, whose lateral diffusion is measured, is labeled exclusively by monovalent Fab' (with Cy3-GαM Fab' as a secondary antibody). In control experiments without myc-TβRIII cross-linking, the IgG labeling of myc-TβRIII was replaced by exclusive Fab' labeling (replacing the cross-linking IgGs by their respective Fab' fragments). The lateral mobility of the Fab'-labeled HA-ALK1 was measured by FRAP at 15°C with or without IgG cross-linking of myc-TβRIII. (E) Average R_f values. (F) Average D values. Bars are mean ± SEM; the number of measurements (each conducted on a different cell) is depicted on each bar. Some of these numbers are lower in panel E because FRAP curves yielding less than 20% recovery could be accurately analyzed only for R_f. Asterisks indicate significant differences between the R_f values of the pairs indicated by brackets (*, $P < 0.01$; ***, $P < 10^{-9}$; Student's two-tailed t test). No significant differences were found between D values as a result of IgG cross-linking of TβRIII. While Neither the D nor the R_f values were significantly affected by the addition of TGF-β1 or -β2 ligands, BMP9 reduced the ALK1 R_f value.

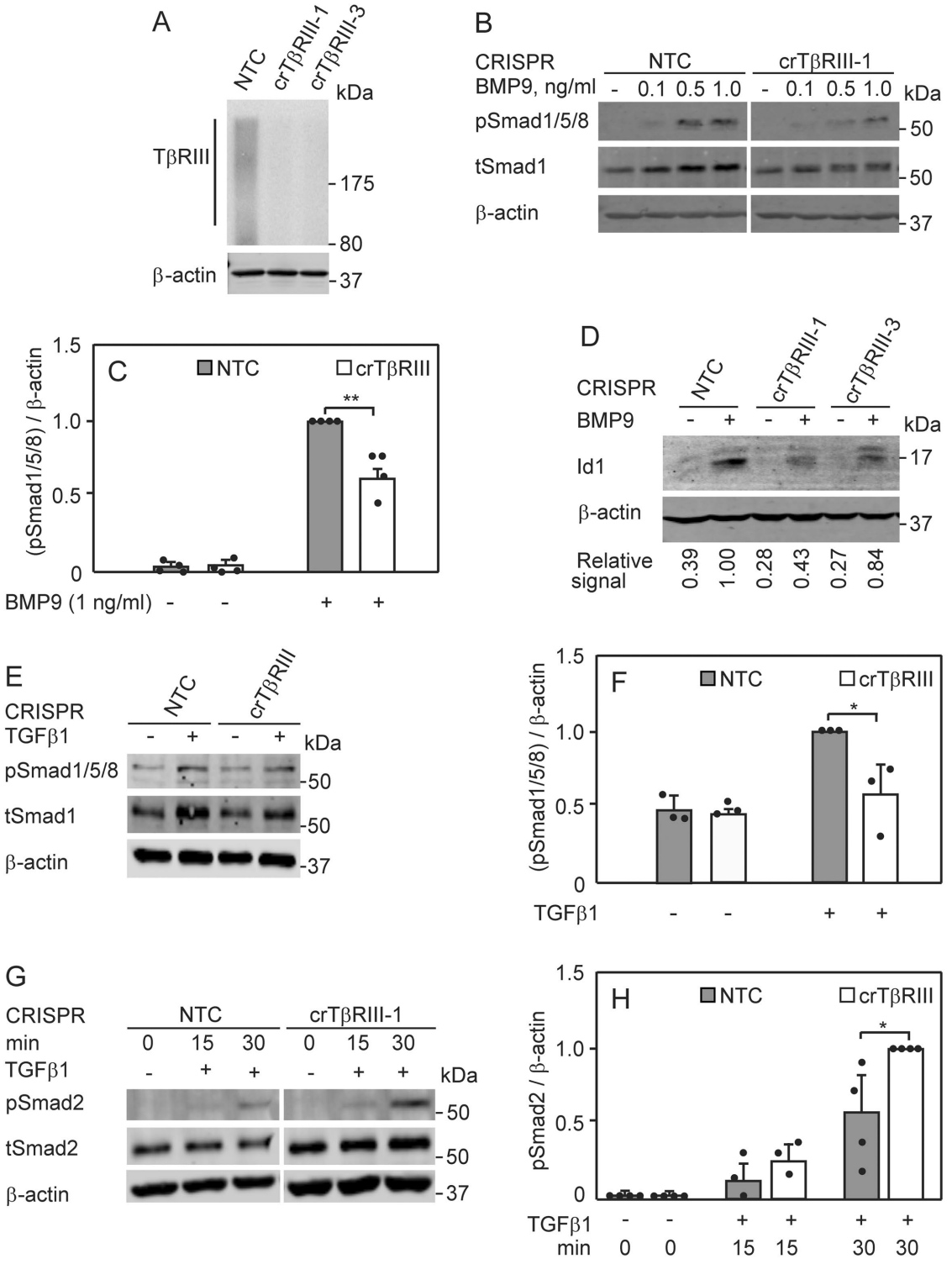

FIGURE 3: TβRIII facilitates Smad1/5/8 phosphorylation induced by BMP9 or TGF-β1 and inhibits TGF-β1–mediated pSmad2 formation. (A) CRISPR silencing of TβRIII in MEECs. CRISPR knockout of TβRIII employed stable transduction with lentivirus, using nontargeting guide sequences for control (NTC; see *Materials and Methods*). Cell surface TβRIII was detected by [^{125}I]TGF-β1 binding/cross-linking followed by immunoprecipitation. A representative experiment (n = 3) is shown. (B–H) Effects of TβRIII knockout in MEECs on signaling to distinct Smad pathways. MEECs transduced with CRISPR-mediated TβRIII knockout (crTβRIII cells) or with NTC lentivirus (control; NTC cells) were compared. After overnight serum starvation, cells were treated with BMP9 or TGF-β1 as indicated, lysed, and analyzed by immunoblotting for total (t) and phospho (p) Smad1/5/8 or Smad2, Id1, and β-actin. The bands were quantified by the Odyssey system (see *Materials and Methods*). (B) Representative blot showing that TβRIII knockout reduces BMP9-induced pSmad1/5/8 formation. Stimulation was with increasing doses of BMP9 (15 min). (C) Quantification of the reduction in BMP9-induced pSmad1/5/8 formation following TβRIII knockout. Stimulation was with 1 ng/ml BMP9

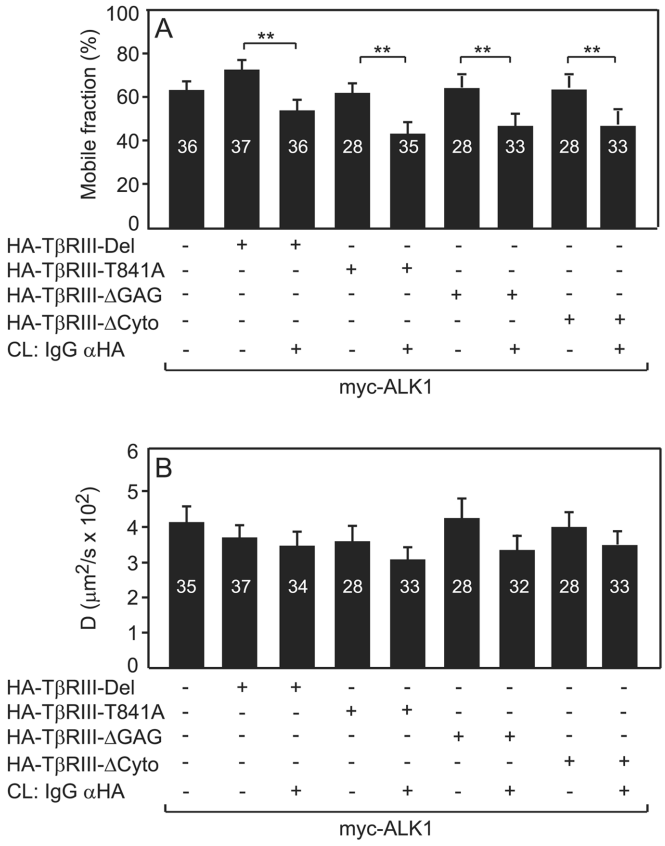

FIGURE 4: The interactions between ALK1 and TβRIII do not depend on the TβRIII cytoplasmic tail or on its glycosylation sites. COS7 cells were cotransfected by myc-ALK1 together with the HA-tagged TβRIII mutants Del, T841A, ΔGAG, ΔCyto or empty vector. They were labeled for patch/FRAP experiments by protocol 1 (*Materials and Methods*) for IgG patching/cross-linking, which leads to immobilization of the HA-tagged TβRIII mutants (cross-linking with rabbit IgG αHA and Alexa 488-DαC IgG). The lateral mobility of Fab'-labeled myc-ALK1 proteins was measured with or without cross-linking of the HA-TβRIII mutants. (A) Average R_f values. (B) Average *D* values. Bars are mean ± SEM; the number of measurements (each conducted on a different cell) is depicted on each bar. Some of these numbers are lower in panel B because FRAP curves yielding less than 20% recovery could be accurately analyzed only for R_f. Asterisks indicate significant differences between the R_f values of the pairs indicated by brackets (**, $P < 0.001$; Student's *t* test). Cross-linking of any of the TβRIII mutants reduced the R_f of myc-ALK1, while its *D* values were not affected, similar to the observations following IgG cross-linking of myc-TβRIII-WT (compare with Figure 2, E and F).

internalization (Figure 6G), in line with a former report (Finger *et al.*, 2008). On the other hand, TβRIII mutations that interfere with its binding to β-arrestin2 (HA-TβRIII-T841A) or GIPC (HA-TβRIII-Del) had no significant effect on TβRIII endocytosis (Figure 6G).

Similar to TβRIII, endoglin exhibited slow endocytosis ($t_{½}$ ~ 35 min), independent of ligand (TGF-β1 or BMP9) (Figure 7, A–F). However, unlike TβRIII, endoglin internalization was partially sensitive to inhibitors of both CME (PitStop 2) and caveolar endocytosis (nystatin) (Figure 7, D–F), indicating that both pathways are involved. As in the case of TβRIII, mutations that interfere with endoglin binding to β-arrestin2 (HA-endoglin-T650A) or GIPC (HA-endoglin-Del) had no effect on endoglin endocytosis (Figure 7G).

The signaling TGF-β receptors, and especially ALK1, enhance endoglin endocytosis

The interactions between endoglin and the signaling TGF-β receptors (TβRII, ALK5, and ALK1) result in the formation of mutual complexes at the cell surface (Pomeraniec *et al.*, 2015), raising the intriguing possibility that they may regulate the endocytosis of the receptors and thus affect their cell surface levels and signaling. Because the endocytosis rate of endoglin is much slower than those of ALK1, ALK5, or TβRII, complex formation between endoglin and these receptors could either increase the rate of endoglin internalization or inhibit the endocytosis rates of the signaling receptors residing in the mutual complexes. To explore these possibilities, we coexpressed HA-endoglin with myc-tagged ALK1, ALK5, or TβRII, labeled the cell surface receptors by fluorescent antibody fragments, and measured HA-endoglin endocytosis in cells coexpressing one of the myc-tagged receptors (Figure 8). Coexpression with any of the signaling TGF-β receptors enhanced the internalization rate of endoglin, with no additional effect by ligand (TGF-β1 or BMP9; Figure 8). The degree of enhancement was correlated with the internalization rate of the coexpressed receptor, with ALK1 (characterized by the fastest endocytosis rate) leading to a twofold faster internalization of HA-endoglin, while ALK5 and TβRII induced a weaker but significant enhancement. The dependence of the effect on the endocytosis rate of the receptor coexpressed with HA-endoglin was validated by coexpression with endocytosis-defective myc-TβRII-HA (Ehrlich *et al.*, 2001), which had the opposite effect and slowed the internalization of endoglin to a half-time of ~70 min (Figure 8). These findings suggest that in the endoglin-TGF-β receptor complexes, the internalization signals of the latter are dominant. In line with this notion, the reciprocal experiment testing the effects of HA-endoglin on the internalization rate of myc-tagged ALK1, ALK5, or TβRII showed no significant effect of endoglin on the endocytosis of any of the latter receptors, in either the absence or presence of ligands (TGF-β1 or BMP9; Figure 9).

(15 min). Results are shown as the pSmad1/5/8 ratio to β-actin, defining the value obtained for BMP9-treated NTC cells as 1. Each bar is the mean ± SEM value of four independent experiments (**, $P < 0.003$; Student's two-tailed *t* test). (D) Loss of TβRIII reduces Id1 induction in response to BMP9. A representative blot ($n = 3$) is shown. Cells (NTC control or TβRIII-silenced) were serum starved overnight and treated with 1 ng/ml BMP9 for 4 h, and the level of Id1 induction was measured by Western blotting. Each Id1 band was calibrated relative to β-actin. The value obtained for BMP9-stimulated NTC cells was defined as 1. (E) Representative blot depicting an increase in TGF-β1–stimulated pSmad1/5/8 formation upon loss of TβRIII. Stimulation (30 min) was with 100 pM TGF-β1. (F) Quantification of TGF-β1–induced pSmad1/5/8 formation. The cells were stimulated with 100 pM TGF-β1 (30 min). Results depict the mean ± SEM of three independent experiments, with the ratio of pSmad1/5/8 to β-actin in NTC cells taken as 1 (*, $P < 0.05$; Student's *t* test). (G) Representative blot depicting an increase in TGF-β1–stimulated pSmad2 formation upon loss of TβRIII. Cells were stimulated by 100 pM TGF-β1 for 15 or 30 min. (H) Quantification of TGF-β1–mediated pSmad2 formation. The ratio of pSmad2 to β-actin in TGF-β1–stimulated crTβRIII cells was taken as 1. Bars, mean ± SEM of three or four independent experiments (*, $P < 0.05$; Student's *t* test).

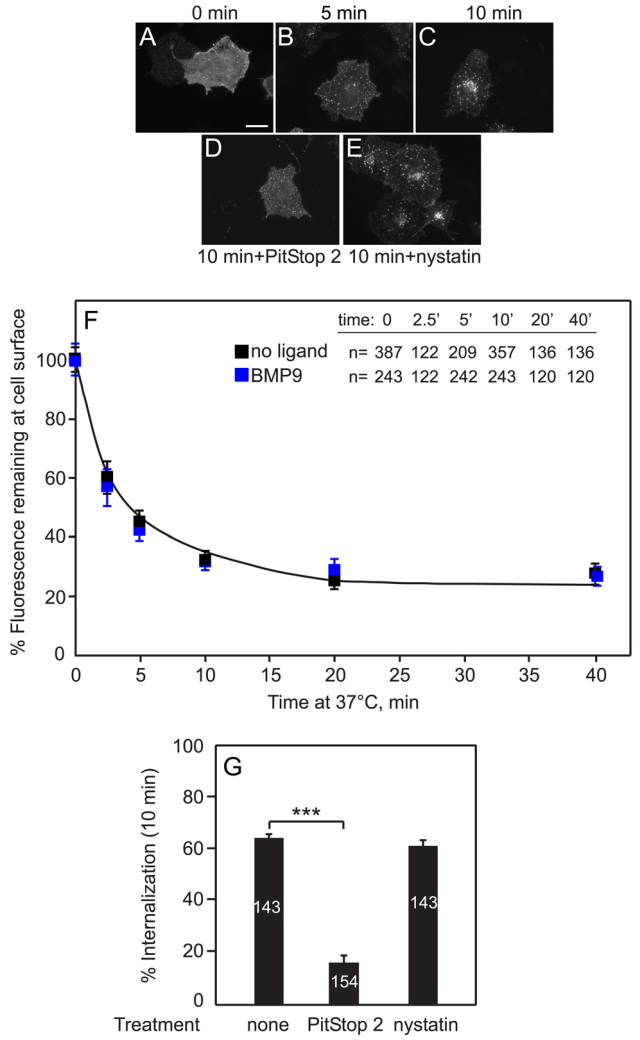

FIGURE 5: ALK1 undergoes fast endocytosis mainly through clathrin-coated pits. COS7 cells were transfected with myc-ALK1. After 24 h, they were either left untreated or subjected to an internalization-inhibiting treatment (PitStop 2 or nystatin). In experiments with ligands, TGF-β1 (250 pM) or BMP9 (5 ng/ml) was added after starvation along with the NGG at the start of the fluorescence labeling procedure (see *Materials and Methods*) and maintained during the following labeling and endocytosis steps. The surface receptors on live cells were then labeled at 4°C (time zero) with mouse αmyc followed by Alexa 546-GαM Fab', incubated for defined intervals at 37°C, returned to 4°C, and fixed (*Materials and Methods*). (A–E) Typical images of myc-ALK1 internalization. Bar, 20 μm. The incubation time at 37°C is designated for each panel. Panels D and E depict cells treated to inhibit CME (PitStop 2) or caveolar endocytosis (nystatin), respectively. (F) Quantitative measurements of the endocytosis of myc-ALK1. The fluorescence intensity remaining at the cell surface was measured by the point-confocal method (*Materials and Methods*), focusing the laser beam on defined spots in the plasma membrane focal plane, away from vesicular staining. Results are mean ± SEM; the number of measurements (each conducted on a different cell) is depicted in a table within the panel. For each sample, the intensity at time zero was taken as 100%. Because incubation with either TGF-β1 or BMP9 had no effect on ALK1 internalization, only the results of one such treatment (BMP9) are shown. (G) ALK1 internalization is inhibited by PitStop 2 but not by nystatin. At 24 h posttransfection, cells were left untreated or treated with either PitStop 2 or nystatin (see *Materials and Methods*). The surface receptors were then labeled at 4°C, followed by a 20 min incubation at 37°C or 4°C (time zero) in media containing inhibitors where indicated. Endocytosis of myc-ALK1 was quantified by the point-confocal method. Results are mean ± SEM; the number of measurements at 10 min is depicted on each bar. For each treatment, the fluorescence intensity of the same sample at time zero ($n = 167$, 159, and 134 for untreated, PitStop 2-treated, or nystatin-treated cells, respectively) was taken as 100%. The percentage of the fluorescence intensity remaining at the cell surface after 10 min at 37°C was subtracted to obtain the % internalization. Treatment with PitStop 2, which inhibits CME, significantly reduced the ALK1 endocytosis (***, $P < 10^{-12}$; Student's two-tailed *t* test), while nystatin had no significant effect.

ALK1 but not ALK5 or TβRII enhances the endocytosis of TβRIII

Because ALK1, ALK5, and TβRII form complexes with TβRIII (Tazat *et al.*, 2015, and Figures 2 and 4), we next explored the effects of these receptors (myc-tagged) on HA-TβRIII endocytosis. As shown in Figure 10, the pattern of these effects was different from that exerted on the endocytosis of endoglin. While coexpression with ALK1 significantly increased the internalization rate of TβRIII, ALK5 and TβRII had no significant effects on TβRIII endocytosis, in either the absence or presence of ligands (Figure 10). These results imply that in the mutual complexes with TβRIII, the endocytosis signal of ALK1 prevails, but this is not the case for the complexes of TβRIII with ALK5 or TβRII. The results of mirror experiments testing the effects of HA-TβRIII coexpression on the internalization rates of myc-tagged ALK1, ALK5, or TβRII are in complete agreement with this suggestion (Figure 11). Thus, if the ALK1 endocytosis signal in the TβRIII-ALK1 complex is dominant, it is expected that endoglin would not affect ALK1 endocytosis, as is indeed the case (with or without ligand). On the other hand, the endocytosis rates of ALK5 and TβRII, which do not enhance TβRIII internalization, are inhibited by coexpressed TβRIII (Figure 11), suggesting that the endocytosis signal of the latter receptor (which undergoes slow endocytosis) is dominant in the complexes with ALK5 or TβRII.

Given the differential regulation of endocytosis of the various receptors involved in BMP9 signaling in ECs, we tested whether disruption of either CME or caveolar endocytosis in MEECs (which express all the receptors studied here) affects Smad1/5/8 activation by BMP9. As shown in Figure 12, the CME inhibitor PitStop 2 significantly inhibited pSmad1/5/8 formation, while the caveolar inhibitor nystatin had no effect. These findings suggest that CME is required for BMP9 signaling to Smad1/5/8 in these cells and are in line with CME being the major pathway for endocytosis of ALK1 (the signal transducing receptor in this setting) and of most of the other TGF-β family receptors studied here.

DISCUSSION

Interactions between multiple TGF-β signaling receptors and coreceptors are at the core of TGF-β superfamily signaling (Seki *et al.*, 2003; Shi and Massague, 2003; Lebrin *et al.*, 2004; Derynck and Miyazono, 2008; Ehrlich *et al.*, 2012; Heldin and Moustakas, 2016). ECs coexpress distinct TGF-β receptors (ALK1, ALK5, TβRII), as well as the coreceptors endoglin (Jonker and Arthur, 2002; Lebrin *et al.*, 2005) and TβRIII (Morello *et al.*, 1995; Brown *et al.*, 1999; see Figure 1). The signaling output of TGF-β receptors is determined by the composition and cellular localization of heteromeric receptor complexes (Ehrlich *et al.*, 2012; Ehrlich, 2016). Typically, the cellular localization of transmembrane receptors is regulated by molecular determinants (e.g., endocytic motifs), which mediate their inclusion

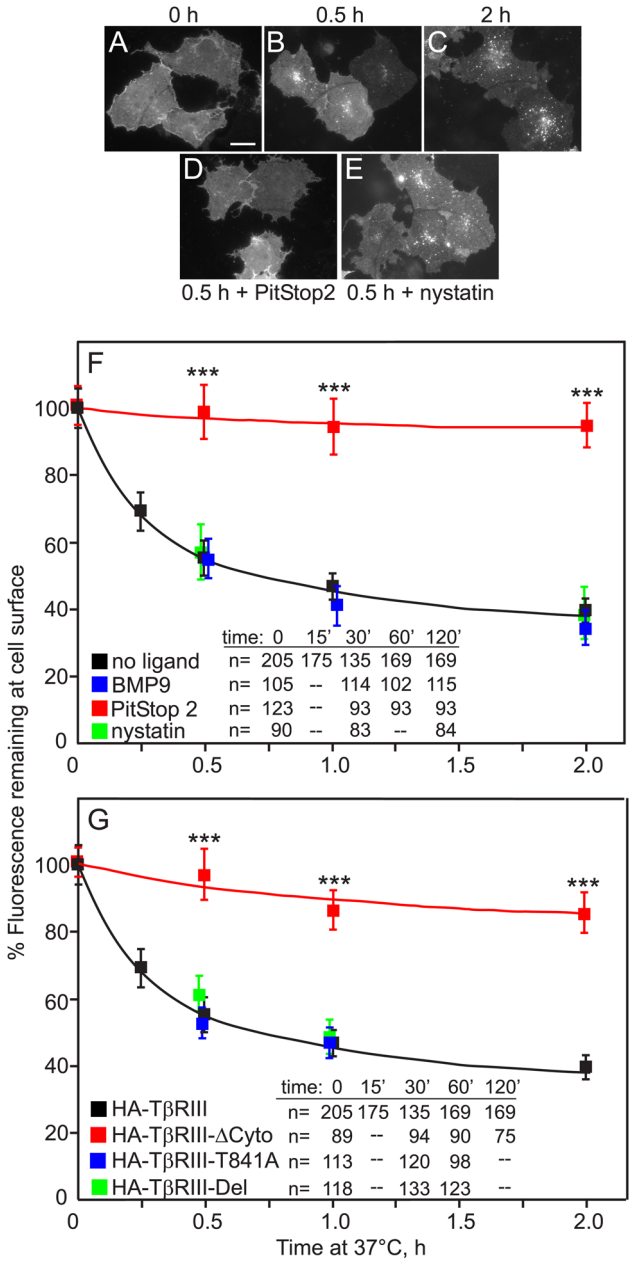

FIGURE 6: TβRIII undergoes slow endocytosis via clathrin-coated pits, which depends on its short cytoplasmic tail. COS7 cells were transfected with HA-TβRIII, HA-TβRIII-ΔCyto, HA-TβRIII-Del, or HA-TβRIII-T841A. After 24 h, they were either left untreated or subjected to an internalization-inhibiting treatment (PitStop 2 or nystatin). In experiments with ligands, TGF-β1 (250 pM) or BMP9 (5 ng/ml) was added after starvation along with the NGG at the start of the fluorescence labeling procedure (see *Materials* and *Methods*) and maintained during the following labeling and endocytosis steps. The surface receptors on live cells were then labeled at 4°C (time zero) with monoclonal mouse αHA followed by Alexa 546-GαM Fab', incubated for defined intervals at 37°C, returned to 4°C, and fixed (*Materials and Methods*). (A–E) Typical images of HA-TβRIII internalization. Bar, 20 μm. The incubation time at 37°C is designated for each panel. Panels D and E depict cells treated to inhibit CME (PitStop 2) or caveolar endocytosis (nystatin), respectively. (F) Quantitative measurements of HA-TβRIII endocytosis. The fluorescence intensity remaining at the cell surface was measured by the point-confocal method (*Materials and Methods*) as described for Figure 5. Results are mean ± SEM; the number of measurements (each conducted on a different cell) is depicted in a table within the panel. For each sample, the intensity at time zero was taken as 100%. Because incubation with either TGF-β1 or BMP9 had no effect on HA-TβRIII internalization, only the results of one ligand (BMP9) are shown. Asterisks indicate significant differences at a given time point between drug-treated and untreated cells (***, $P < 10^{-12}$; Student's two-tailed *t* test). (G) The short cytoplasmic tail of TβRIII is required for its endocytosis. Experiments were conducted as in panel F, comparing the internalization rates of WT HA-TβRIII (shown in this panel as well for reference) with those of the designated mutants. Results are mean ± SEM; the number of measurements is depicted in a table within the panel. Asterisks indicate significant differences at a given time point between a mutant and the WT HA-TβRIII (***, $P < 10^{-12}$; Student's *t* test). The HA-TβRIII-ΔCyto mutant, which misses most of the cytoplasmic domain, exhibited defective endocytosis, while deletion of only the last three amino acids (HA-TβRIII-Del) or point mutation to interfere with binding to β-arrestin2 (HA-TβRIII-T841A) had no significant effects.

into trafficking intermediates such as clathrin-coated pits (Ohno *et al.*, 1995; Ehrlich, 2016; Heldin and Moustakas, 2016). The coexpression of multiple TGF-β receptor types highlights the importance of studying their interactions, and the formation of multimeric receptor complexes raises the possibility of reciprocal influence between complex formation, endocytosis, and signaling. While complex formation between endoglin or TβRIII with the signaling TGF-β receptors was reported (Pomeraniec *et al.*, 2015; Tazat *et al.*, 2015), the interactions of ALK1 with TβRIII were not investigated, and the endocytosis of ALK1 was not described. Moreover, the potential effects of complex formation, especially with ALK1 (which we now find to undergo CME at the fastest rate among TGF-β receptors), on endocytosis and signaling remained unexplored. Here we show that ALK1 forms stable, ligand-independent complexes with TβRIII, similar to those reported for ALK1-endoglin (Pomeraniec *et al.*, 2015). We find that complex formation alters the internalization rates of the participating receptors, depending on the complex formed. Our findings lead to a model (Figure 13) in which the endocytosis signal of ALK1 is dominant in complexes with either coreceptor, while ALK5 and TβRII endocytosis motifs are exposed/active in complexes with endoglin, but not with TβRIII. Moreover, the different levels of the mRNA transcripts for these receptors in different EC types suggest that the extent of their mutual interactions and the resulting effects on signaling provide an additional level of cell-specific regulation. These findings have implications for TGF-β signaling in ECs.

We have formerly demonstrated heteromeric complex formation between TβRI and TβRII, as well as between TβRIII or endoglin and the signaling TGF-β receptors (Henis *et al.*, 1994; Gilboa *et al.*, 1998; Rechtman *et al.*, 2009; Ehrlich *et al.*, 2012; Pomeraniec *et al.*, 2015; Tazat *et al.*, 2015). However, although ALK1 was shown to interact with endoglin with effects on its signaling (Pomeraniec *et al.*, 2015), no such data were available for the interactions of ALK1 with TβRIII. The present patch/FRAP and coimmunoprecipitation studies (Figure 2) clearly demonstrate interactions between the two receptors. These interactions are stable on the FRAP timescale, because cross-linking and immobilization of myc-TβRIII reduced the R_f of HA-ALK1 without affecting its diffusion rate (Figure 2) and were independent of ligands (TGF-β1, TGF-β2, BMP9), ALK1 kinase activity, the TβRIII cytoplasmic domain (including mutations defective in β-arrestin2 or GIPC binding), and TβRIII glycosylation (Figures 2 and

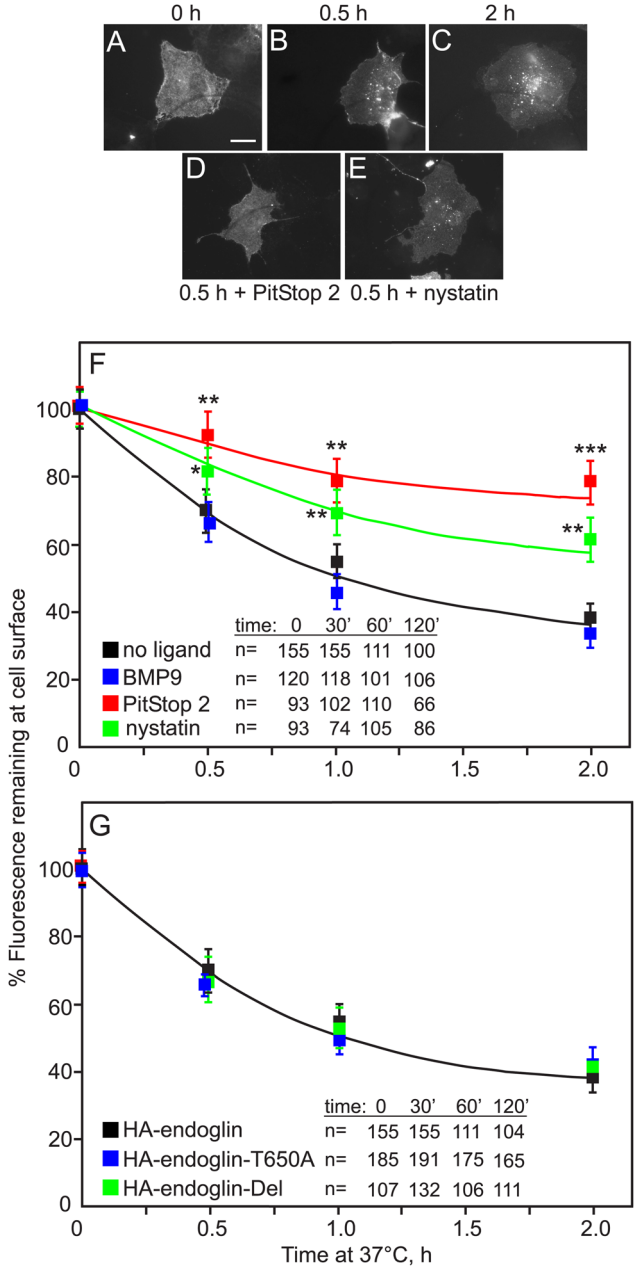

FIGURE 7: The slow endocytosis of endoglin proceeds via both clathrin-coated pits and a nystatin-sensitive pathway. Experiments were conducted exactly as in Figure 6, except that the receptors whose endocytosis was followed were HA-endoglin (WT) or its HA-tagged mutants HA-endoglin-Del and HA-endoglin-T650A. (A–E) Typical images of HA-endoglin endocytosis. Bar, 20 μm. The incubation time at 37°C is designated for each panel. Panels D and E depict cells treated to inhibit CME (PitStop 2) or caveolar endocytosis (nystatin), respectively. (F) Quantitative measurements of HA-endoglin endocytosis, measured by the point-confocal method as described for Figures 5 and 6. Results are mean ± SEM; the number of measurements (each conducted on a different cell) is depicted in a table within the panel. The intensity at time zero for each sample was taken as 100%. Because incubation with either TGF-β1 or BMP9 had no effect on HA-TβRIII internalization, only the results of one ligand (BMP9) are shown. Asterisks indicate significant differences at a given time point between drug-treated and untreated cells (*, $P < 0.01$; **; $P < 10^{-3}$; ***, $P < 10^{-12}$; Student's *t* test). (G) Endoglin endocytosis does not depend on interactions with GIPC or β-arrestin2. Experiments were as in panel F, comparing the internalization rates of WT HA-endoglin (shown in this panel again for reference) with the designated mutants. Results are mean ± SEM; the number of measurements is depicted in a table within the panel. No significant differences were observed in the internalization of the endoglin mutants as compared with WT endoglin.

4). Similar features (stable complex formation with no dependence on ligand, cytoplasmic domain of the coreceptor or mutations in this domain) were reported for the interactions of endoglin with ALK1 and for the interactions of both endoglin and TβRIII with TβRII or ALK5 (Pomeraniec *et al.*, 2015; Tazat *et al.*, 2015). Of note, the TβRIII-ALK1 interactions reported here modulate ALK1 signaling, as demonstrated by the reduced BMP9 or TGF-β1 signaling to Smad1/5/8 upon silencing of TβRIII (Figure 3, B–E). These effects are distinct from those exerted via ALK5, as shown by the increased pSmad2 formation in response to TGF-β1 in TβRIII knockout MEECs (Figure 3, G and H).

The coexpression and mutual complex formation among the multiple TGF-β receptors and coreceptors motivated us to explore whether these interactions can modulate their endocytosis. To this end, we studied the endocytosis of the different receptors under similar conditions and in the same cells, using the same method (point-confocal internalization measurements) employed earlier to measure ALK5 and TβRII endocytosis (Ehrlich *et al.*, 2001; Shapira *et al.*, 2012). We find that ALK1 undergoes constitutive internalization mainly via CME, in line with our earlier studies on the endocytosis of TβRII, ALK5, and the long form of BMPRII (Ehrlich *et al.*, 2001; Shapira *et al.*, 2012; Amsalem *et al.*, 2016). In this context, it should be noted that while the endocytosis pathways of the type I and II TGF-β receptors have been controversial due to contrasting data and methods, the current near-consensus is that CME is their main internalization pathway (Ehrlich *et al.*, 2001; Hayes *et al.*, 2002; Penheiter *et al.*, 2002; Yao *et al.*, 2002; Di Guglielmo *et al.*, 2003; Mitchell *et al.*, 2004; Chen, 2009), possibly complemented by a contribution from caveolar-like endocytosis (Ehrlich *et al.*, 2001; Hayes *et al.*, 2002; Penheiter *et al.*, 2002; Yao *et al.*, 2002; Di Guglielmo *et al.*, 2003; Mitchell *et al.*, 2004; Chen, 2009). However, ALK1 endocytosis is significantly faster (approximately fivefold) than that of ALK5 or TβRII (Figure 5) and is therefore potentially important for modulating the endocytosis of interacting receptors and for signaling. Indeed, blockade of CME by PitStop 2 inhibited pSmad1/5/8 formation following BMP9 stimulation in MEECs (Figure 12), in line with a role for endocytosis in the modulation of this signaling pathway. On the other hand, under the same conditions, the coreceptors TβRIII and endoglin undergo significantly slower endocytosis. For TβRIII, the internalization was found to proceed mainly via CME (Figure 6F), in line with some studies but not with others (Finger *et al.*, 2008; McLean and Di Guglielmo, 2010). The current studies show no dependence of TβRIII endocytosis on its T841 site (Figure 6G), which binds β-arrestin2. This differs from our prior report, which measured internalized iodinated TGF-β1 after 2 h (Chen *et al.*, 2003). This apparent discrepancy may stem from methodological differences, as the current studies focus on direct measurement of the internalization of the T841 mutant. Moreover, we now find that the slow internalization of endoglin is insensitive to mutations that interfere with its ability to bind β-arrestin2 or GIPC (Figure 7G). This finding is seemingly at odds with our earlier reports on the effects of these mutations on the

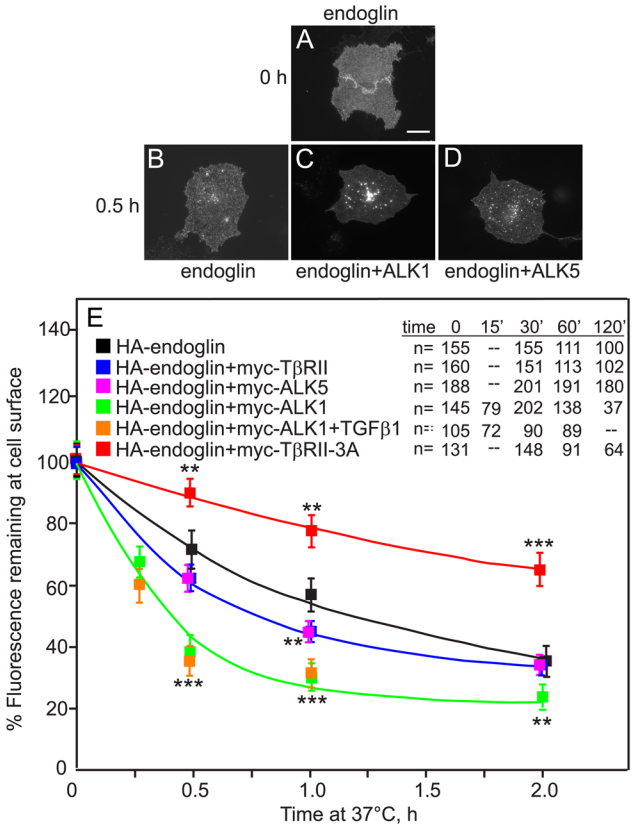

FIGURE 8: Endoglin endocytosis is enhanced strongly by ALK1 and mildly by ALK5 or TβRII. COS7 cells were transfected with HA-endoglin alone or together with another myc-tagged receptor (myc-ALK1, myc-ALK5, myc-TβRII, or its endocytosis-defective myc-TβRII-3A mutant). The HA-tagged receptors were labeled with rabbit monoclonal HA.11 αHA (20 μg/ml, 45 min, 4°C) followed by Alexa 546-GαR Fab′ (40 μg/ml, 45 min, 4°C); coexpression of the myc-tagged receptors was validated by labeling in parallel with murine αmyc followed by Alexa 488-GαM Fab′. Endocytosis studies were conducted as in Figure 6. (A–D) Typical images of HA-endoglin internalization. Bar, 20 μm. The incubation time at 37°C (0 or 30 min) is indicated to the left of the panels. (A, B) Cells expressing HA-endoglin alone; (C, D) HA-endoglin coexpressed with myc-ALK1 or myc-ALK5, respectively. (E) Quantitative measurements of HA-endoglin endocytosis, measured by the point-confocal method (see Figure 6). Coexpression with ALK1 enhanced markedly the internalization rate of HA-endoglin, while ALK5 or TβRII induced a mild effect in the same direction, suggesting that the stronger endocytosis signal of the receptors complexed with endoglin is exposed in the complex and prevails. This notion is supported by the reverse effect of the endocytosis-defective TβRII-3A mutant. The effect of ligands (250 pM TGF-β1 or 5 ng/ml BMP9) was insignificant for HA-endoglin endocytosis in combination with any of the receptors; thus, for simplicity, only the effect of TGF-β1 on the internalization of HA-endoglin in the presence of myc-ALK1 is shown. Results are mean ± SEM; the number of measurements is depicted in a table within the panel. The intensity of the same sample at time zero was taken as 100%. Asterisks indicate significant differences between HA-endoglin endocytosis in the presence of the depicted coexpressed receptor and the value measured for singly expressed HA-endoglin at the same time point (**; $P < 1\ 0^{-6}$; ***, $P < 10^{-12}$; Student's *t* test).

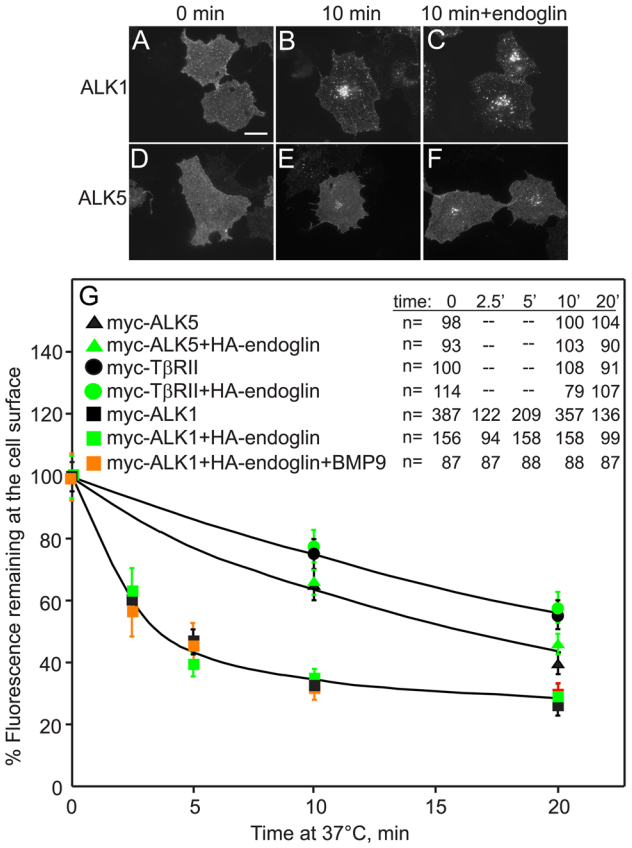

FIGURE 9: Endoglin expression does not affect the endocytosis of the signaling TGF-β receptors. COS7 cells were transfected with myc-tagged ALK1, ALK5, or TβRII alone or together with HA-endoglin. The myc-tagged receptors were labeled with murine monoclonal αmyc (20 μg/ml, 45 min, 4°C) followed by Alexa 546-GαM Fab′ (40 μg/ml, 45 min, 4°C); coexpression of HA-endoglin was validated by labeling in parallel with HA.11 rabbit αHA followed by Alexa 488-GαR Fab′. The effect of HA-endoglin coexpression on the internalization of the myc-tagged receptors was measured by the point-confocal method, as described in Figure 6. (A–F) Representative images of myc-ALK1 (top row) or myc-ALK5 (bottom row) internalization; HA-endoglin was coexpressed in panels C and F. Bar, 20 μm. The incubation time at 37°C (time 0 or 10 min) is indicated above the top panels. (G) Quantitative point-confocal measurements of myc-ALK1, myc-ALK5, or myc-TβRII endocytosis. No significant effect of HA-endoglin on the endocytosis of any of the other receptors was observed. Addition of ligand (250 pM TGF-β1 or 5 ng/ml BMP9) had no effect on the endocytosis of either myc-ALK5, myc-TβRII, or myc-ALK1 coexpressed with HA-endogin; for simplicity, only the effect of one ligand (BMP9) on the internalization of myc-ALK1 is shown. Results are mean ± SEM; the number of measurements is depicted in a table within the panel. Endoglin had no significant effects on the internalization of ALK1, TβRII, or ALK5.

cell surface levels of the endoglin mutants (Lee and Blobe, 2007; Lee *et al.*, 2008). However, the earlier reports measured the cell surface steady state levels of endoglin, while the current studies specifically assessed endoglin internalization.

Complex formation between receptors that undergo fast versus slow endocytosis can modulate their internalization. Depending on the special conformation acquired by the cytoplasmic domains in the complex, the cytoplasmic endocytosis signals of one receptor or both may be sequestered from interacting with the endocytic machinery. If the endocytosis signals of both receptors remain functional in the complex, the fast internalization rate of the fast-endocytosed receptor is expected to prevail. A similar scenario of functional prevalence of the strong endocytosis signal is expected when this signal is exposed while the weaker counterpart (of the slow-endocytosed receptor) is sequestered (e.g., as in

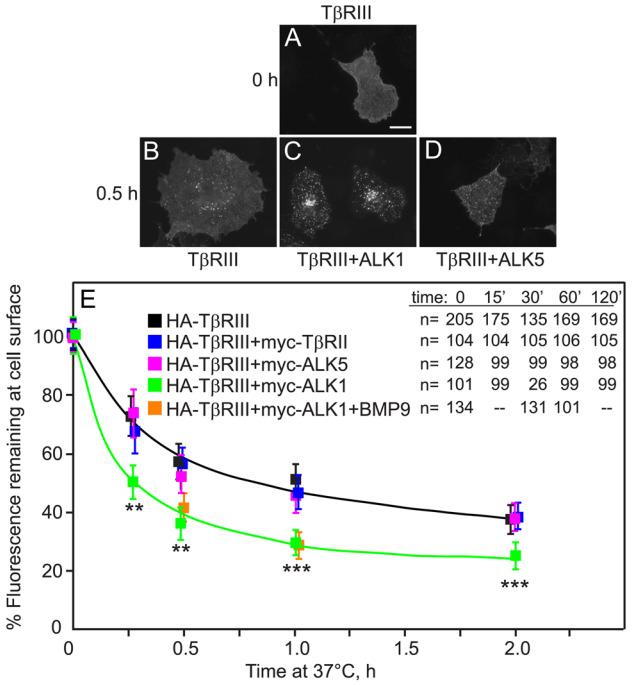

FIGURE 10: ALK1, but not ALK5 or TβRII, enhances the endocytosis rate of TβRIII. COS7 cells were transfected with HA-TβRIII together with myc-ALK5, myc-TβRII, or myc-ALK1. The cellsurface receptors were labeled exactly as in Figure 8 and subjected to endocytosis studies following the internalization of HA-TβRIII as in Figure 8. All studies were repeated also with ligand (250 pM TGF-β1 or 5 ng/ml BMP9), which in all cases had no effect (for simplicity, shown only for HA-TβRIII coexpressed with myc-ALK1 and measured in the presence of BMP9). (A–D) Typical images of the internalization of HA-TβRIII alone (A, B) or coexpressed with myc-ALK1 (C) or myc-ALK5 (D). Bar, 20 μm. The incubation time at 37°C is indicated to the left of the panels. (E) Quantitative point-confocal endocytosis measurements of HA-TβRIII. Results are mean ± SEM; the number of measurements is depicted in a table within the panel. For each sample, the intensity at time zero was taken as 100%. Asterisks indicate significant differences between HA-TβRIII endocytosis in the presence of coexpressed myc-ALK1 and the value measured for singly expressed HA-TβRIII at the same time point (**; $P < 10^{-3}$; ***, $P < 5 \times 10^{-5}$; Student's *t* test).

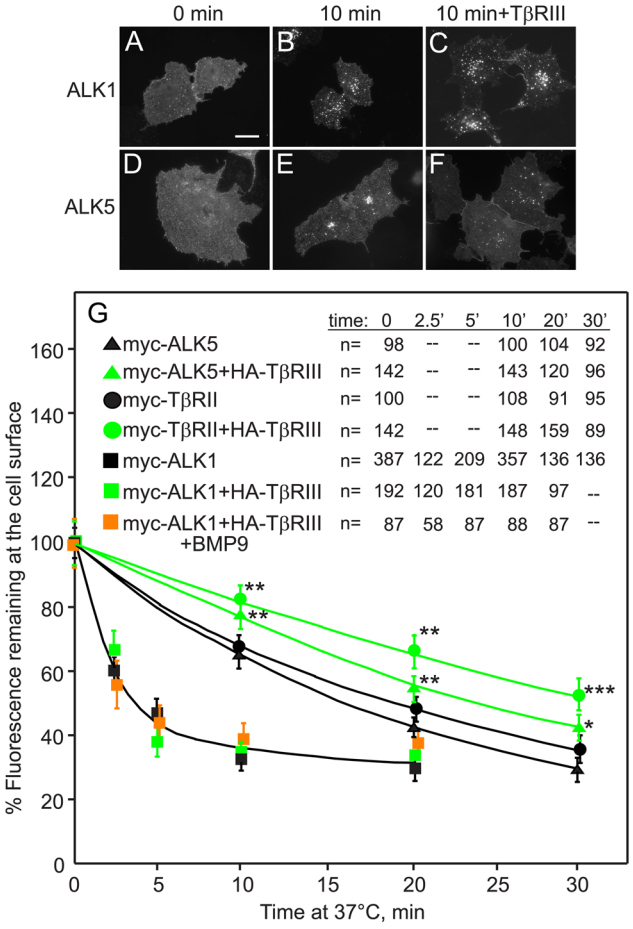

FIGURE 11: TβRIII inhibits the endocytosis of TβRII and ALK5, but not that of ALK1. COS7 cells were transfected with myc-tagged TβRII, ALK5, or ALK1 alone or together with HA-TβRIII. The cell surface receptors were labeled exactly as in Figure 9, and the internalization of the myc-tagged receptors was measured by the point-confocal method as in Figure 9. Addition of ligand (250 pM TGF-β1 or 5 ng/ml BMP9) had no effect on the endocytosis of any of the myc-tagged receptors coexpressed with HA-TβRIII; for simplicity, only the results of myc-ALK1 internalization in the presence of HA-TβRIII with one ligand (BMP9) are shown. (A–F) Typical images of myc-ALK1 (top row) and myc-ALK5 (bottom row) internalization; HA-TβRIII was coexpressed in panels C and F. Bar, 20 μm. The incubation time at 37°C (time 0 or 10 min) is indicated above the top panels. (G) Quantitative point-confocal measurements of myc-ALK1, myc-ALK5, or myc-TβRII endocytosis. Results are mean ± SEM; the number of measurements is depicted in a table within the panel. Asterisks indicate significant differences between the internalization of a given myc-tagged receptor without (black symbols) and with (green symbols) coexpressed HA-TβRIII at the same time point (*, $P < 0.01$; **; $P < 10^{-4}$; ***, $P < 10^{-12}$; Student's *t* test).

the complexes of ALK1-endoglin or ALK1-TβRIII; Figure 13). Conversely, in cases in which the strong signal is sequestered and the weak signal is the sole determinant of the internalization rate, slower internalization of the receptor complex is expected. In accord with this model, the internalization rates of TβIII or endoglin complexed with ALK1 were significantly enhanced (Figures 8 and 10), while the endocytosis rate of ALK1 was unaffected by complex formation with either of these receptors (Figure 9). These findings indicate that the strong endocytosis signal of ALK1 predominates in these complexes (Figure 13). It should be noted that the elevation in the internalization rate of TβRIII or endoglin by ALK1 does not reach the fast-endocytosis rate of singly expressed ALK1; this is in line with the fact that only a certain percentage of the receptor population resides in mutual complexes. The endocytosis signal of the faster-endocytosed receptor appears to prevail also for the complexes of endoglin with TβRII or ALK5, because these signaling receptors also enhance endoglin endocytosis, albeit to a lower degree than ALK1 (Figure 8). Of note, the opposite effect (reduction in the internalization rate of endoglin) due to complex formation with an endocytosis-defective TβRII mutant (TβRII-3A; Figure 8) suggests that the weak endocytosis signal of endoglin is sequestered in this complex (Figure 13). A different scenario is observed for TβRIII complexes with TβRII or ALK5. Here, TβRII or ALK5 failed to affect TβRIII endocytosis (Figure 10), suggesting that their endocytosis signals are sequestered in the complex. Concomitantly, TβRIII was able to slow the internalization of TβRII and ALK5 (Figure 11). Thus, within such complexes, the signal that determines the internalization of the complex is that of TβRIII (Figure 13).

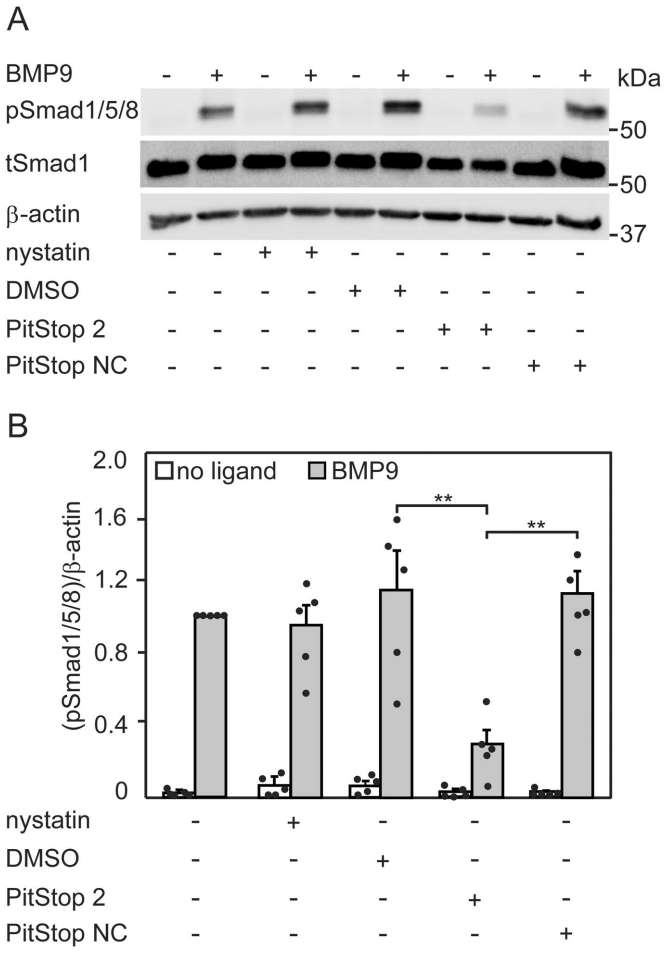

FIGURE 12: CME blockage inhibits BMP9 signaling in MEECs. (A) Immunoblot analysis of BMP9-induced Smad1/5/8 activation. MEECs were serum starved overnight and treated (or not) with an endocytosis inhibitor (25 μg/ml nystatin or 30 μM PitStop 2, 15 min, 37°C). Vehicle (0.5% dimethyl sulfoxide) or the inactive negative control of PitStop 2 (PitStop NC) was employed as a control. Cells were stimulated (or not) with BMP9 (1 ng/ml, 30 min), lysed, and analyzed by immunoblotting for pSmad1/5/8, total Smad1, and β-actin. The blot depicts a typical experiment ($n = 5$). (B) Quantification of pSmad1/5/8 formation. The graph depicts the mean ± SEM of the pSmad1/5/8 over β-actin ratio of five independent experiments. The value obtained for BMP9-stimulated untreated cells was defined as 1. Asterisks indicate a significant difference between the pairs indicated by brackets (**, $P < 0.01$; Student's two-tailed *t* test).

Taken together, these studies provide further insight into another mechanism for regulating TGF-β superfamily signaling and downstream biology, which may also be relevant to signaling by receptors from other families that form specific complexes. Of note, the different expression levels of distinct receptors in different cells and organs have potential functional implications, because the effects of complex formation among the different interacting receptors on their endocytosis and signaling are expected to depend on their surface expression levels. As the function and expression of the TGF-β superfamily receptors studied here are altered in many human diseases, including HHT and cancer, how these alterations affect the trafficking and signaling of other TGF-β superfamily receptors to contribute to the pathophysiology of these diseases remains an active area of exploration.

MATERIALS AND METHODS

Reagents

Recombinant human TGF-β1 (cat. #100-21C) was from PeproTech (Rocky Hill, NJ). Recombinant human BMP9 (cat. #3209-BP-010) and goat IgG against the extracellular domain of TβRIII (cat. #AF-242-PB) were from R&D Systems (Minneapolis, MN). Protein G-Sepharose (cat. #P3296) and mouse anti–β-actin (cat. #A2228) were from Sigma-Aldrich (St. Louis, MO), and disuccinimidyl suberate (DSS; cat. #21655) was from Thermo Scientific Pierce (Grand Island, NY). Fatty acid free bovine serum albumin (BSA) (fraction V; cat. #10-775-835-001) and 12CA5 murine monoclonal anti-influenza hemagglutinin tag (αHA) IgG (cat. #11-66-606-001) were obtained from Roche Diagnostics (Manheim, Germany). Murine monoclonal anti-myc tag (αmyc; cat. #626802) 9E10 IgG (Evan *et al.*, 1985) and HA.11 rabbit polyclonal IgG to the HA tag (rabbit αHA; cat. #923502) were from Biolegend (San Diego, CA). Monovalent Fab' fragments were prepared from the 9E10 and 12CA5 IgG as described (Henis *et al.*, 1994). Chicken anti-myc tag affinity-purified IgY (cat. #AB3252) was from Merck Millipore (Burlington, MA). Alexa Fluor (Alexa) 488-GαR IgG (cat. #R37116), Alexa 488-GαR F(ab')$_2$ (cat. #A-11070), and Alexa 546-goat anti-mouse (GαM) F(ab')$_2$ (cat. #A-11018) were from Invitrogen-Molecular Probes (Eugene, OR). Normal goat γ-globulin (cat. #005-000-002), Cy3 conjugated AffiniPure GαM F(ab')$_2$ (cat. #115-166-146), and Alexa 488-conjugated AffiniPure donkey IgG against chicken IgY (DαC; cat. #703-545-155) were from Jackson ImmunoResearch Laboratories (West Grove, PA). Fluorescent F(ab')$_2$ was converted to Fab' as described (Gilboa *et al.*, 1998). Rabbit antibodies to phospho (p) Smad1/5/8 (cat. #9511), total (t) Smad1 (cat. #9743), and phospho (p) Smad2 (cat. #19338), as well as murine antibody to total (t) Smad 2 (cat. #3103) and infrared-tagged secondary donkey IgG against rabbit (DαR 800; cat. #5151) or mouse (DαM 680; cat. #5470) were from Cell Signaling Technology (Danvers, MA). Rabbit antibodies to Id1 (C-20) (cat. #sc-488) were from Santa Cruz Biotechnology (Santa Cruz, CA). [^{125}I]TGF-β1 (cat. #NEX267010UC) was from PerkinElmer (Waltham, MA). PitStop 2 (cat. # ab120687) was obtained from Abcam (Cambridge, United Kingdom), and nystatin suspension (cat. # 03-030) was from Biological Industries Israel.

Plasmids

Expression vectors encoding WT human TβRI (in pcDNA3) or TβRII (in pcDNA1) with extracellular myc or HA epitope tags, as well as HA-TβRIII or myc-TβRIII in pcDNA3, were described by us earlier (Henis *et al.*, 1994; Gilboa *et al.*, 1998; Ehrlich *et al.*, 2001; Chetrit *et al.*, 2009; Tazat *et al.*, 2015). HA- or myc-tagged ALK1, HA-ALK1-Q201D (constitutively active point mutant), and HA-ALK1-K221R (kinase dead mutant) in pcDNA3.1 (Nakao *et al.*, 1997; Lee and Blobe, 2007; Tian *et al.*, 2012) were a gift from D. A. Marchuk (Duke University, Durham, NC). HA-TβRIII-ΔCyto (truncated after IYSD, lacking most of the cytoplasmic domain), HA-TβRIII-Del (lacking the last three C-terminal amino acids comprising a class I PDZ binding domain, resulting in loss of binding to GIPC), HA-TβRIII-T841A (a point mutation that abrogates TβRIII binding to β-arrestin2), and HA-TβRIII-ΔGAG (lacking the two glycosaminoglycan attachment sites) in pcDNA3.1 were described (Blobe *et al.*, 2001; Chen *et al.*, 2003; Kirkbride *et al.*, 2008). HA-tagged endoglin (endoglin-L), HA-endoglin-Del (lacking the last three C-terminal amino acids, resulting in loss of binding to GIPC), and HA-endoglin-T650A (a point mutation that abrogates endoglin binding to β-arrestin2) in pDisplay were described (Lee and Blobe, 2007; Lee *et al.*, 2008), as well as untagged endoglin and myc-tagged endoglin in pcDNA3.1 (Pomeraniec *et al.*, 2015).

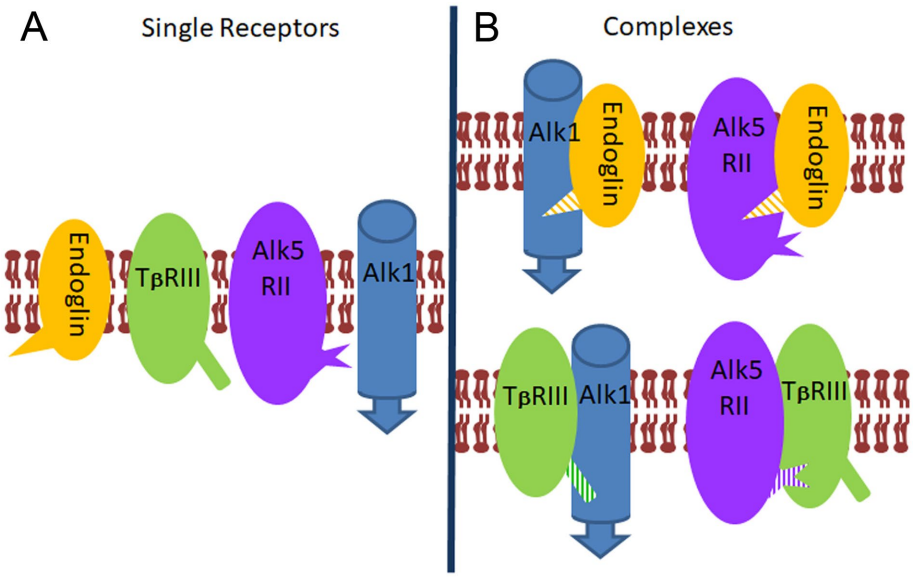

FIGURE 13: Model for the effects of complex formation between endoglin or TβRIII and signaling TGF-β receptors on their internalization. All receptors are drawn as monomers for simplicity. The endocytosis signals specific to each receptor (wide arrow for ALK1, triangle for endoglin, rectangle for TβRIII, dovetail for ALK5 or TβRII) are designated with full color when they are exposed and active and with stripes when the signal is inactive (sequestered) in the complex. Uncomplexed receptors (A) are internalized by virtue of their specific endocytosis signals (fast endocytosis of ALK1, medium rate for ALK5 or TβRII, and slow for endoglin or TβRIII). When mutual complexes are formed between these receptors (B), the internalization rate of the complex is determined by which endocytosis signals are exposed/active or masked/sequestered. Thus, the endocytosis signal of ALK1 is dominant in complexes with either endoglin or TβRIII, resulting in enhanced internalization of the latter two coreceptors. On the other hand, the endocytosis signals of ALK5 and TβRII are exposed/active in complexes with endoglin (enhancing endoglin internalization, albeit to a lower degree than ALK1 due to their weaker endocytosis signals), but not with TβRIII. As a result, ALK5 or TβRII does not enhance TβRIII internalization, while TβRIII slows the endocytosis of ALK5 or TβRII.

Cell culture and transfection

COS7 cells (cat. #CRL-1651) from the American Type Culture Collection (ATCC; Manassas, VA) were grown in DMEM with 10% fetal calf serum (Biological Industries Israel, Beit Haemek, Israel) as described (Gilboa *et al.*, 1998; Shapira *et al.*, 2012). MEECs from endoglin WT (MEEC$^{+/+}$) mice (Pece-Barbara *et al.*, 2005; a gift from E. Dejana, University of Milan, Italy) were grown on 0.02% gelatin-coated plates in MCDB-131 medium (Invitrogen, Thermo Fisher Scientific, Carlsbad, CA) supplemented with 10% fetal calf serum, 2 mM L-glutamine, 1 mM sodium pyruvate, 100 μg/ml heparin (Sigma-Aldrich), and 50 μg/ml EC growth supplement (Sigma-Aldrich). All cells were routinely analyzed by reverse transcriptase-PCR (RT-PCR) for mycoplasma contamination and found to be clean.

For patch/FRAP experiments and endocytosis studies, COS7 cells were grown on glass coverslips in six-well plates and transfected by TransIT-LT1 transfection reagent (Mirus Bio LLC, Madison, WI) with different combinations of vectors encoding myc- and HA-tagged (or untagged) receptor constructs. For endoglin, which expresses at higher levels than the TGF-β receptors, 300 ng plasmid DNA was used per transfection, while the DNA amounts of the vectors encoding the various TGF-β receptors were adjusted to yield similar cell surface expression levels (around 0.5 μg), determined by quantitative immunofluorescence as described by us earlier (Marom *et al.*, 2011). The total DNA level was complemented by empty vector to 2 μg.

IgG-mediated patching/cross-linking

At 24 h posttransfection, COS7 cells transfected with various combinations of expression vectors for endoglin and TGF-β receptors were serum starved (30 min, 37°C), washed with cold Hank's balanced salt solution (HBSS; Biological Industries Israel) supplemented with 20 mM HEPES (pH 7.4) and 2% BSA (HBSS/HEPES/BSA), and blocked with normal goat γ-globulin (200 μg/ml, 30 min, 4°C). They were then labeled successively at 4°C (to avoid internalization and enable exclusive cell surface labeling) in HBSS/HEPES/BSA (45 min incubations) with 1) monovalent mouse Fab' αmyc (40 μg/ml) together with HA.11 rabbit αHA IgG (20 μg/ml) and 2) Alexa 546-Fab' GαM (40 μg/ml) together with Alexa 488-IgG GαR (20 μg/ml). This protocol (protocol 1) results in the HA-tagged receptor cross-linked and immobilized by IgGs, whereas the myc-tagged receptor, whose lateral diffusion is then measured by FRAP, is labeled exclusively by monovalent Fab'. Alternatively, for immobilizing the myc-tagged receptor and measuring the lateral diffusion of a coexpressed Fab'-labeled HA-tagged receptor, the labeling protocol used (protocol 2) was 1) monovalent mouse Fab' αHA (40 μg/ml) together with chicken IgY αmyc (20 μg/ml) and 2) Cy3-Fab' GαM (40 μg/ml) together with Alexa 488-IgG DαC (20 μg/ml). This protocol results in the myc-tagged receptor being immobilized and the HA-tagged receptor labeled by monovalent Fab'. In experiments with TGF-β1 or BMP9, the ligands (250 pM TGF-β1 or 5 ng/ml BMP9) were added after starvation along with the normal goat γ-globulin and maintained at this concentration during the following labeling steps and FRAP measurements.

FRAP and patch/FRAP

Cells coexpressing epitope-tagged receptors labeled fluorescently by anti-tag Fab' fragments as described above were subjected to FRAP and patch/FRAP studies as described by us earlier (Rechtman *et al.*, 2009; Pomeraniec *et al.*, 2015; Tazat *et al.*, 2015). FRAP studies were conducted at 15°C, replacing samples after 20 min to minimize internalization during the measurement. An argon-ion laser beam (Innova 70C; Coherent, Santa Clara, CA) was focused through a fluorescence microscope (Axioimager.D1; Carl Zeiss MicroImaging, Jena, Germany) to a Gaussian spot of 0.77 ± 0.03 μm (Planapochromat 63×/1.4 NA oil-immersion objective). After a brief measurement at monitoring intensity (528.7 nm, 1 μW), a 5 mW pulse (20 ms) bleached 60–75% of the fluorescence in the illuminated region, and fluorescence recovery was followed by the monitoring beam. Values of D and R_f were extracted from the FRAP curves by nonlinear regression analysis, fitting to a lateral diffusion process (Petersen *et al.*, 1986). Patch/FRAP studies were performed similarly, except that IgG-mediated cross-linking-patching of an epitope-tagged TGF-β receptor or endoglin (described above) preceded the measurement (Henis *et al.*, 1990;

Rechtman *et al.*, 2009; Pomeraniec *et al.*, 2015). This enables determination of the effects of immobilizing one receptor type on the lateral diffusion of the coexpressed receptor (labeled exclusively with monovalent Fab'), allowing identification of complex formation between the receptors and distinction between transient and stable interactions (Henis *et al.*, 1990; Rechtman *et al.*, 2009; Tazat *et al.*, 2015).

Internalization measurements

COS7 cells grown on glass coverslips in six-well plates were transfected as described for the IgG cross-linking and FRAP studies. After serum starvation (30 min, 37°C), they were blocked with NGG (200 µg/ml, 30 min, 4°C) and labeled with mouse monoclonal αmyc or αHA IgG (20 µg/ml, 45 min, 4°C) followed by Alexa 546-GαM Fab' (40 µg/ml, 45 min, 4°C), all in HBSS/HEPES/BSA. In experiments in which the effects of another, differently tagged receptor (e.g., HA-tagged) on the internalization of the measured receptor (e.g., myc-tagged) were measured, coexpression of the HA-tagged receptor was validated by labeling in parallel with rabbit monoclonal HA.11 followed by Alexa 488-GαR Fab'. In experiments with TGF-β1 (250 pM) or BMP9 (5 ng/ml), the ligands were added after starvation along with the NGG and maintained during the following labeling and endocytosis steps. The internalization of the tagged receptors was quantified by the point-confocal method employing the FRAP setup under nonbleaching illumination conditions (Ehrlich *et al.*, 2001; Shapira *et al.*, 2012). Labeled cells were either fixed immediately with 4% paraformaldehyde or warmed to 37°C for the indicated periods to allow endocytosis; they were then transferred back to 4°C, fixed, and mounted for immunofluorescence as above. Endocytosis was quantified by measuring the reduction in the fluorescence intensity levels at the plasma membrane, focusing the laser beam through the 63× objective at defined spots (1.86 μm^2) in the focal plane of the plasma membrane away from vesicular staining, passing the fluorescence through a pinhole in the image plane to make it a true confocal measurement (Ehrlich *et al.*, 2001).

Treatments affecting internalization

Endocytosis assays involving the use of inhibitors were initiated by a 15-min preincubation (37°C) with the inhibitory drug. The cells were kept under the inhibitory condition throughout the labeling and internalization measurement. Nystatin treatment to inhibit caveolar endocytosis (Schnitzer *et al.*, 1994; Di Guglielmo *et al.*, 2003; Mitchell *et al.*, 2004) employed 25 µg/ml drug. Treatment with the clathrin inhibitor PitStop 2 was at 30 µM (von Kleist *et al.*, 2011).

CRISPR to silence TβRIII expression in ECs

CRISPR knockout of MEECs was achieved by stable transduction with lentivirus from puromycin-expressing pLentiCRISPRV2 constructs (Addgene Plasmid 52961; Addgene, Watertown, MA) subcloned with guide RNAs targeting murine TβRIII, or nontargeting control (NTC) guide sequences from the GeCKov2 database (Heckl *et al.*, 2014; Shalem *et al.*, 2014). Targeting sequences used were Ms crNTC, MGLibA_66406, GCGAGGTATTCGGCTCCGCG; Ms crTβRIII-1, MGLibA_53624, CTTCAACCCAAAGCCGCCGA; Ms crTβRIII-3, MGLibA_53626, AACCTCCGCAGTACAGACCA. Viral particles were made by cotransfecting the subcloned CRISPR vectors bearing Cas9 and the guide sequences with virus packaging plasmids psPAX2 and pMD2.G in 293FT cells. Media was changed after 24 h, and the viral supernatants were collected at 48 and 72 h posttransfection, filtered through 0.45 micron membranes, and stored at –80°C or used immediately. Infection of target cells was achieved by incubation with 8 µg/ml polybrene for 24–48 h. Cells were allowed to recover in regular growth media for at least 24 h before selection in puromycin and analysis for gene expression or other experimental procedures.

Western blotting and coimmunoprecipitation

MEECs plated in six-well dishes were serumstarved overnight in MCDB-131 media, followed by incubation with ligands (BMP9 or TGF-β1) for the indicated times and doses. They were then lysed in 2× sample buffer and subjected to electrophoresis on 10% SDS–PAGE followed by immunoblotting. The blots were probed by rabbit anti-pSmad1/5/8 (1:500), rabbit anti-Smad1 (1:1000), rabbit anti-pSmad2 (1:1000), mouse anti-Smad2 (1:1000), or mouse anti–β-actin (1:10,000), followed by Cell Signaling DαR 800 or DαM 680 (1:5000) infrared-tagged secondary antibodies. The bands were visualized by the Odyssey Classic infrared imaging system and quantified by LI-COR Image Studio software (both from LI-COR Biotechnology, Lincoln, NE).

For coimmunoprecipitation, COS7 cells coexpressing HA- or myc-tagged TβRIII and ALK1 were washed with phosphate-buffered saline and lysed on ice with RIPA buffer (150 mM NaCl, 1% Nonidet P40, 0.1% SDS, 50 mM Tris/HCl, pH 7.4, 0.5% sodium deoxycholate, 1 mM EDTA, and 10 mM sodium phosphate) supplemented with protease inhibitors (0.2 mM phenylmethylsulfonyl fluoride, 10 µg/ml pepstatin, 10 µg/ml leupeptin, 5 mM dithiothreitol). Lysates were centrifuged (20 min, 4°C), and the supernatants were incubated overnight with protein G-Sepharose beads and antibody as indicated. Beads were washed three times with HNTG buffer (20 mM HEPES, pH 7.5, 0.15 M NaCl, 0.1% Triton X-100, 10% glycerol) and boiled in 1× sample buffer before Western blot analysis.

Iodinated ligand binding and cross-linking

Cells grown in six-well plates were incubated with 100 pM [^{125}I] TGF-β-1 in the presence of fatty acid–free BSA and protease inhibitors (3 h, 4°C). The ligand was then cross-linked to the receptors using 0.5 mg/ml DSS and quenched with 20 mM glycine. Cells were lysed with RIPA buffer supplemented with protease inhibitors. Ligand–receptor complexes were immunoprecipitated overnight at 4°C using goat IgG directed against the extracellular domain of TβRIII. The resulting complexes were separated by SDS–PAGE (7.5% polyacrylamide), and dried gels were subjected to autoradiography with Typhoon 9200 Variable mode Imager (Molecular Dynamics, Pittsburgh, PA). Images were analyzed using ImageJ (National Institutes of Health, Bethesda, MD).

RT-PCR and RT-qPCR

Total RNA was isolated from cells grown in six-well plates using the Qiagen RNAEasy kit (cat. #74104; Qiagen, Hilden, Germany), and cDNA synthesis was performed using the iScript cDNA Synthesis Kit (cat. #170-8891; Bio-Rad, Hercules, CA). The expression of TβRIII in several human and murine cell lines was determined by RT-PCR with GAPDH as loading control, using the iQ SYBR Green SuperMix (cat. #170-882; Bio-Rad) and the following primers: 1) murine TβRIII—5′-GGTGTGAACTGTC-ACCGATCA-3′ (forward) and 5′- GTTTAGGAT-GTGAACCTCCCTTG-3′ (reverse); 2) human TβRIII—5′- CTGTT-CACCCGACCTGAAAT-3′ (forward) and 5′-CGTCAGGAGG-CACA-CACTTA-3′ (reverse); 3) murine GAPDH—5′-GTCTACATGTT-CCAGTATGACTCC-3′ (forward) and 5′-AGTGAGTTGTCATA-TTTCTCGTGGT-3′ (reverse); and 4) human GAPDH—5′-GAGT-CAACGGATTTGTCGT-3′ (forward) and 5′-TTGATTTTGGAGGG-ATCTCG-3′ (reverse).

To quantify the transcript mRNA levels of TβRIII, endoglin, and ALK1 in several human cell lines, we employed RT-qPCR. RNA isolation and cDNA synthesis were carried out as above. Using the iQ SYBR Green SuperMix in a BioRad iCycler, relative mRNA levels were determined by the comparative threshold cycle (C_T) method (Livak and Schmittgen, 2001), normalizing the data to GAPDH. The RT-qPCR data (run in triplicate in each experiment) were analyzed using the BioRad CFX Connect real-time system software. For human TβRIII and human GAPDH, the primers used were those described above for RT-PCR. For human endoglin, the primers were 5′-AGTGAAGCCTCTGAGGGATTG-3′ (forward) and 5′-GCCATATCCCAGACCCACTG-3′ (reverse). For human ALK1, the primers were 5′-GCCACCCAACCTCCTTCGG-3′ (forward) and 5′-ACACACTCCACCAAGGCAAC-3′ (reverse).

ACKNOWLEDGMENTS

This work was supported by grant 2013011 from the United States–Israel Binational Science Foundation (BSF) (to Y.I.H. and G.C.B.) and by grant R01CA236843 from the National Institutes of Health/National Cancer Institute (to G.C.B.). Y.I.H. is an incumbent of the Zalman Weinberg Chair in Cell Biology.

REFERENCES

Alt A, Miguel-Romero L, Donderis J, Aristorena M, Blanco FJ, Round A, Rubio V, Bernabeu C, Marina A (2012). Structural and functional insights into endoglin ligand recognition and binding. PLoS One 7, e29948.

Amsalem AR, Marom B, Shapira KE, Hirschhorn T, Preisler L, Paarmann P, Knaus P, Henis YI, Ehrlich M (2016). Differential regulation of translation and endocytosis of alternatively spliced forms of the type II bone morphogenetic protein (BMP) receptor. Mol Biol Cell 27, 716–730.

Arthur HM, Ure J, Smith AJ, Renforth G, Wilson DI, Torsney E, Charlton R, Parums DV, Jowett T, Marchuk DA, *et al*. (2000). Endoglin, an ancillary TGFβ receptor, is required for extraembryonic angiogenesis and plays a key role in heart development. Dev Biol 217, 42–53.

Bernabeu C, Lopez-Novoa JM, Quintanilla M (2009). The emerging role of TGF-β superfamily coreceptors in cancer. Biochim Biophys Acta 1792, 954–973.

Blobe GC, Liu X, Fang SJ, How T, Lodish HF (2001). A novel mechanism for regulating transforming growth factor β (TGF-β) signaling. Functional modulation of type III TGF-β receptor expression through interaction with the PDZ domain protein, GIPC. J Biol Chem 276, 39608–39617.

Bourdeau A, Dumont DJ, Letarte M (1999). A murine model of hereditary hemorrhagic telangiectasia. J Clin Invest 104, 1343–1351.

Brown CB, Boyer AS, Runyan RB, Barnett JV (1999). Requirement of type III TGF-β receptor for endocardial cell transformation in the heart. Science 283, 2080–2082.

Budi EH, Duan D, Derynck R (2017). Transforming growth factor-β receptors and Smads: regulatory complexity and functional versatility. Trends Cell Biol 27, 658–672.

Chen W, Kirkbride KC, How T, Nelson CD, Mo J, Frederick JP, Wang XF, Lefkowitz RJ, Blobe GC (2003). β-Arrestin 2 mediates endocytosis of type III TGF-β receptor and down-regulation of its signaling. Science 301, 1394–1397.

Chen YG (2009). Endocytic regulation of TGF-β signaling. Cell Res 19, 58–70.

Chen YG, Massague J (1999). Smad1 recognition and activation by the ALK1 group of transforming growth factor-β family receptors. J Biol Chem 274, 3672–3677.

Chetrit D, Ziv N, Ehrlich M (2009). Dab2 regulates clathrin assembly and cell spreading. Biochem J 418, 701–715.

Compton LA, Potash DA, Brown CB, Barnett JV (2007). Coronary vessel development is dependent on the type III transforming growth factor β receptor. Circ Res 101, 784–791.

Derynck R, Miyazono K (2008). TGF-β and the TGF-β family. In: The TGF-*β* Family, ed. R. Derynck and K. Miyazono, New York: Cold Spring Harbor Laboratory Press, 29–43.

Di Guglielmo GM, Le Roy C, Goodfellow AF, Wrana JL (2003). Distinct endocytic pathways regulate TGF-β receptor signalling and turnover. Nat Cell Biol 5, 410–421.

Ehrlich M (2016). Endocytosis and trafficking of BMP receptors: regulatory mechanisms for fine-tuning the signaling response in different cellular contexts. Cytokine Growth Factor Rev 27, 35–42.

Ehrlich M, Gutman O, Knaus P, Henis YI (2012). Oligomeric interactions of TGF-β and BMP receptors. FEBS Lett 586, 1885–1896.

Ehrlich M, Shmuely A, Henis YI (2001). A single internalization signal from the di-leucine family is critical for constitutive endocytosis of the type II TGF-β receptor. J Cell Sci 114, 1777–1786.

Eickelberg O, Centrella M, Reiss M, Kashgarian M, Wells RG (2002). Betaglycan inhibits TGF-β signaling by preventing type I-type II receptor complex formation: glycosaminoglycan modifications alter betaglycan function. J Biol Chem 277, 823–829.

Eisenberg S, Shvartsman DE, Ehrlich M, Henis YI (2006). Clustering of raft-associated proteins in the external membrane leaflet modulates internal leaflet H-Ras diffusion and signaling. Mol Cell Biol 26, 7190–7200.

Evan GI, Lewis GK, Ramsay G, Bishop JM (1985). Isolation of monoclonal antibodies specific for human c-myc proto-oncogene product. Mol Cell Biol 5, 3610–3616.

Feng XH, Derynck R (2005). Specificity and versatility in TGF-β signaling through Smads. Annu Rev Cell Dev Biol 21, 659–693.

Finger EC, Lee NY, You HJ, Blobe GC (2008). Endocytosis of the type III TGF-β receptor through the clathrin-independent/lipid raft pathway regulates TGF-β and receptor downregulation. J Biol Chem 283, 34808–34818.

Gatza CE, Oh SY, Blobe GC (2010). Roles for the type III TGF-β receptor in human cancer. Cell Signal 22, 1163–1174.

Gilboa L, Wells RG, Lodish HF, Henis YI (1998). Oligomeric structure of type I and type II TGF-β receptors: homo-dimers form in the ER and persist at the plasma membrane. J Cell Biol 140, 767–770.

Goumans MJ, Lebrin F, Valdimarsdottir G (2003). Controlling the angiogenic switch: a balance between two distinct TGF-β receptor signaling pathways. Trends Cardiovasc Med 13, 301–307.

Goumans MJ, Liu Z, ten Dijke P (2009). TGF-β signaling in vascular biology and dysfunction. Cell Res 19, 116–127.

Hayes S, Chawla A, Corvera S (2002). TGF-β receptor internalization into EEA1-enriched early endosomes: role in signaling to Smad2. J Cell Biol 158, 1239–1249.

Heckl D, Kowalczyk MS, Yudovich D, Belizaire R, Puram RV, McConkey ME, Thielke A, Aster JC, Regev A, Ebert BL (2014). Generation of mouse models of myeloid malignancy with combinatorial genetic lesions using CRISPR-Cas9 genome editing. Nat Biotechnol 32, 941–946.

Heldin CH, Landstrom M, Moustakas A (2009). Mechanism of TGF-β signaling to growth arrest, apoptosis, and epithelial-mesenchymal transition. Curr Opin Cell Biol 21, 166–176.

Heldin CH, Moustakas A (2016). Signaling receptors for TGF-β family members. Cold Spring Harb Perspect Biol 8, a022053.

Henis YI, Katzir Z, Shia MA, Lodish HF (1990). Oligomeric structure of the human asialoglycoprotein receptor: nature and stoichiometry of mutual complexes containing H1 and H2 polypeptides assessed by fluorescence photobleaching recovery. J Cell Biol 111, 1409–1418.

Henis YI, Moustakas A, Lin HY, Lodish HF (1994). The types II and III transforming growth factor-β receptors form homo-oligomers. J Cell Biol 126, 139–154.

Johnson DW, Berg JN, Baldwin MA, Gallione CJ, Marondel I, Yoon SJ, Stenzel TT, Speer M, Pericak-Vance MA, Diamond A, *et al*. (1996). Mutations in the activin receptor-like kinase 1 gene in hereditary haemorrhagic telangiectasia type 2. Nat Genet 13, 189–195.

Jonker L, Arthur HM (2002). Endoglin expression in early development is associated with vasculogenesis and angiogenesis. Mech Dev 110, 193–196.

Kamaid A, Molina-Villa T, Mendoza V, Pujades C, Maldonado E, Ispizua Belmonte JC, Lopez-Casillas F (2015). Betaglycan knock-down causes embryonic angiogenesis defects in zebrafish. Genesis 53, 583–603.

Kirkbride KC, Townsend TA, Bruinsma MW, Barnett JV, Blobe GC (2008). Bone morphogenetic proteins signal through the transforming growth factor-β type III receptor. J Biol Chem 283, 7628–7637.

Lambert KE, Huang H, Mythreye K, Blobe GC (2011). The type III transforming growth factor-β receptor inhibits proliferation, migration, and adhesion in human myeloma cells. Mol Biol Cell 22, 1463–1472.

Lebrin F, Deckers M, Bertolino P, Ten Dijke P (2005). TGF-β receptor function in the endothelium. Cardiovasc Res 65, 599–608.

Lebrin F, Goumans MJ, Jonker L, Carvalho RL, Valdimarsdottir G, Thorikay M, Mummery C, Arthur HM, ten Dijke P (2004). Endoglin promotes endothelial cell proliferation and TGF-β/ALK1 signal transduction. EMBO J 23, 4018–4028.

Lee NY, Blobe GC (2007). The interaction of endoglin with β-arrestin2 regulates transforming growth factor-β-mediated ERK activation and migration in endothelial cells. J Biol Chem 282, 21507–21517.

Lee NY, Ray B, How T, Blobe GC (2008). Endoglin promotes transforming growth factor β-mediated Smad 1/5/8 signaling and inhibits endothelial

cell migration through its association with GIPC. J Biol Chem 283, 32527–32533.
Li DY, Sorensen LK, Brooke BS, Urness LD, Davis EC, Taylor DG, Boak BB, Wendel DP (1999). Defective angiogenesis in mice lacking endoglin. Science 284, 1534–1537.
Livak KJ, Schmittgen TD (2001). Analysis of relative gene expression data using real-time quantitative PCR and the $2^{-\Delta\Delta;CT}$ method. Methods 25, 402–408.
Lopez Casillas F, Payne HM, Andres JL, Massague J (1994). Betaglycan can act as a dual modulator of TGF-β access to signaling receptors: mapping of ligand binding and GAG attachment sites. J Cell Biol 124, 557–568.
Mahmoud M, Borthwick GM, Hislop AA, Arthur HM (2009). Endoglin and activin receptor-like-kinase 1 are co-expressed in the distal vessels of the lung: implications for two familial vascular dysplasias, HHT and PAH. Lab Invest 89, 15–25.
Marom B, Heining E, Knaus P, Henis YI (2011). Formation of stable homomeric and transient heteromeric bone morphogenetic protein (BMP) receptor complexes regulates Smad protein signaling. J Biol Chem 286, 19287–19296.
McAllister KA, Grogg KM, Johnson DW, Gallione CJ, Baldwin MA, Jackson CE, Helmbold EA, Markel DS, McKinnon WC, Murrell J, *et al*. (1994). Endoglin, a TGF-β binding protein of endothelial cells, is the gene for hereditary haemorrhagic telangiectasia type 1. Nat Genet 8, 345–351.
McDonald J, Wooderchak-Donahue W, VanSant Webb C, Whitehead K, Stevenson DA, Bayrak-Toydemir P (2015). Hereditary hemorrhagic telangiectasia: genetics and molecular diagnostics in a new era. Front Genet 6, 1–8.
McLean S, Di Guglielmo GM (2010). TGF β (transforming growth factor β) receptor type III directs clathrin-mediated endocytosis of TGF β receptor types I and II. Biochem J 429, 137–145.
Mitchell H, Choudhury A, Pagano RE, Leof EB (2004). Ligand-dependent and -independent TGF-β receptor recycling regulated by clathrin-mediated endocytosis and Rab11. Mol Biol Cell 15, 4166–4178.
Morello JP, Plamondon J, Meyrick B, Hoover R, O'Connor-McCourt MD (1995). Transforming growth factor-β receptor expression on endothelial cells: heterogeneity of type III receptor expression. J Cell Physiol 165, 201–211.
Moustakas A, Heldin CH (2009). The regulation of TGFβ signal transduction. Development 136, 3699–3714.
Nakao A, Imamura T, Souchelnytskyi S, Kawabata M, Ishisaki A, Oeda E, Tamaki K, Hanai J-I, Heldin C-H, Miyazono K, ten Dijke P (1997). TGF-β receptor-mediated signalling through Smad2, Smad3 and Smad4. EMBO J 16, 5353–5362.
Oh SP, Seki T, Goss KA, Imamura T, Yi Y, Donahoe PK, Li L, Miyazono K, ten Dijke P, Kim S, Li E (2000). Activin receptor-like kinase 1 modulates transforming growth factor-β1 signaling in the regulation of angiogenesis. Proc Natl Acad Sci USA 97, 2626–2631.
Ohno H, Stewart J, Fournier MC, Bosshart H, Rhee I, Miyatake S, Saito T, Gallusser A, Kirchhausen T, Bonifacino JS (1995). Interaction of tyrosine-based sorting signals with clathrin-associated proteins. Science 269, 1872–1875.
Pece-Barbara N, Vera S, Kathirkamathamby K, Liebner S, Di Guglielmo GM, Dejana E, Wrana JL, Letarte M (2005). Endoglin null endothelial cells proliferate faster and are more responsive to transforming growth factor β1 with higher affinity receptors and an activated Alk1 pathway. J Biol Chem 280, 27800–27808.
Penheiter SG, Mitchell H, Garamszegi N, Edens M, Dore JJ Jr, Leof EB (2002). Internalization-dependent and -independent requirements for transforming growth factor β receptor signaling via the Smad pathway. Mol Cell Biol 22, 4750–4759.
Petersen NO, Felder S, Elson EL (1986). Measurement of lateral diffusion by fluorescence photobleaching recovery. In: Handbook of Experimental Immunology, ed. D.M. Weir, L.A. Herzenberg, C.C. Blackwell, and L.A. Herzenberg, Edinburgh: Blackwell Scientific Publications, 24.21–24.23.
Pomeraniec L, Hector-Greene M, Ehrlich M, Blobe GC, Henis YI (2015). Regulation of TGF-β receptor hetero-oligomerization and signaling by endoglin. Mol Biol Cell 26, 3117–3127.
Rechtman MM, Nakaryakov A, Shapira KE, Ehrlich M, Henis YI (2009). Different domains regulate homomeric and heteromeric complex formation among type I and type II transforming growth factor-β receptors. J Biol Chem 284, 7843–7852.
Roman BL, Hinck AP (2017). ALK1 signaling in development and disease: new paradigms. Cell Mol Life Sci 74, 4539–4560.
Schmierer B, Hill CS (2007). TGFβ-SMAD signal transduction: molecular specificity and functional flexibility. Nat Rev Mol Cell Biol 8, 970–982.
Schnitzer JE, Oh P, Pinney E, Allard J (1994). Filipin-sensitive caveolae-mediated transport in endothelium: reduced transcytosis, scavenger endocytosis, and capillary permeability of select macromolecules. J Cell Biol 127, 1217–1232.
Seki T, Yun J, Oh SP (2003). Arterial endothelium-specific activin receptor-like kinase 1 expression suggests its role in arterialization and vascular remodeling. Circ Res 93, 682–689.
Shalem O, Sanjana NE, Hartenian E, Shi X, Scott DA, Mikkelson T, Heckl D, Ebert BL, Root DE, Doench JG, Zhang F (2014). Genome-scale CRISPR-Cas9 knockout screening in human cells. Science 343, 84–87.
Shapira KE, Gross A, Ehrlich M, Henis YI (2012). Coated pit-mediated endocytosis of the type I transforming growth factor-β (TGF-β) receptor depends on a di-leucine family signal and is not required for signaling. J Biol Chem 287, 26876–26889.
Shi Y, Massague J (2003). Mechanisms of TGF-β signaling from cell membrane to the nucleus. Cell 113, 685–700.
Srinivasan S, Hanes MA, Dickens T, Porteous ME, Oh SP, Hale LP, Marchuk DA (2003). A mouse model for hereditary hemorrhagic telangiectasia (HHT) type 2. Hum Mol Genet 12, 473–482.
Tazat K, Hector-Greene M, Blobe GC, Henis YI (2015). TβRIII independently binds type I and type II TGF-β receptors to inhibit TGF-β signaling. Mol Biol Cell 26, 3535–3545.
Tian H, Mythreye K, Golzio C, Katsanis N, Blobe GC (2012). Endoglin mediates fibronectin/α5β1 integrin and TGF-β pathway crosstalk in endothelial cells. EMBO J 31, 3885–3900.
Urness LD, Sorensen LK, Li DY (2000). Arteriovenous malformations in mice lacking activin receptor-like kinase-1. Nat Genet 26, 328–331.
von Kleist L, Stahlschmidt W, Bulut H, Gromova K, Puchkov D, Robertson MJ, MacGregor KA, Tomlin N, Pechstein A, Chau N, *et al*. (2011). Role of the clathrin terminal domain in regulating coated pit dynamics revealed by small molecule inhibition. Cell 146, 471–484.
Yao D, Ehrlich M, Henis YI, Leof EB (2002). Transforming growth factor-β receptors interact with AP2 by direct binding to β2 subunit. Mol Biol Cell 13, 4001–4012.